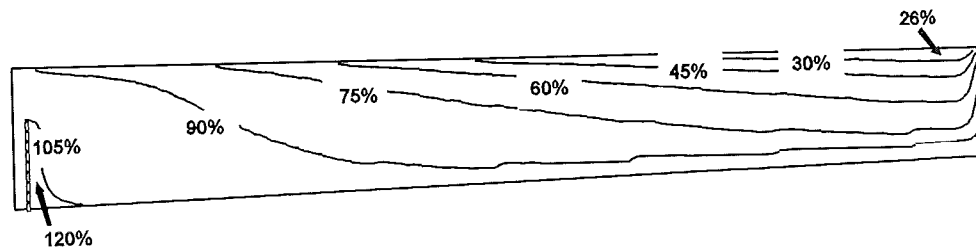


Modelling of flow and settling in storm water sedimentation tanks

Report 5 of the Rionedproject 92-05: research storm water sedimentation tanks.

November 1994

Ir. J. Kluck



Concentration of particles of 0.04 mm in rectangular tank with sloping bottom; inflow concentration = 100%

TABLE OF CONTENTS

1 INTRODUCTION 1

2 MODELLING THE WATER FLOW 2

3 MEASUREMENTS IN A SCALE MODEL 3

 3.1 Experimental setup 3

 3.2 Effect of distance to the bottom on the measurements 5

 3.3 EMS fit 6

 3.4 Zero-measurements 7

4 ANALYSIS OF MEASUREMENTS AND COMPUTATIONS 8

 4.1 Comparison of measurements and computations 8

 4.2 3-D effects 12

5 SEDIMENTATION 16

 5.1 PHOENICS settling model: Algebraic Slip Model 16

 5.2 Uncoupled convective and settling transport 18

 5.3 Uncoupled convective and settling transport with free-surface flow 20

 5.4 Another fully upwind settling method 21

 5.5 Particle size 21

 5.6 Alternative numerical differential schemes 22

6 CONTINUATION OF THE RESEARCH 23

ANNEXES A: REFERENCES 25

ANNEXES C: LIST OF SYMBOLS 26

ANNEXES B: MEASUREMENTS 27

1 INTRODUCTION

In the near future in the Netherlands many reservoirs will have to be built to abate the pollution of the surface water by overflowing storm water from combined sewer systems [Kluck, 1992-a]. These reservoirs, called storm water sedimentation tanks, reduce the pollution in two ways. The most important is by simply storing a part of the sewage (waste water and storm water) and thus reducing the quantity of overflowing water. The second is by providing flow conditions in which particles can settle, so that the overflowing water is less polluted. There are no satisfactory design methods - taking into account the time-varying inflow - for this kind of structures. The aim of the study is to develop design methods for these tanks such that the overall efficiency of the tanks will be optimal. A mathematical model (PHOENICS package) is used to describe the flow and settling in the reservoirs. By using the time-dependent, 2-DV or 3-D mathematical model the effect of changes in lay-out for various shapes of reservoirs can be investigated under variable flows.

The course of this study has been defined as follows: First a mathematical model in which only the water flow is considered will be set up. Computational results will be compared with measurements on a scale model. The flow model will be calibrated with these measurements. Next the particle movement will be modelled. Computations will be compared with experimental data and the model will be calibrated. With the validated model different designs of tanks will be judged and optimal working tanks will be designed.

The work done in the period February 1992 to July 1993 is presented in four reports [Kluck, 1992-a, 1992-b, 1993-a and 1993-b] (written in Dutch). The first report presents the objectives of the research and the present design methods for storm water sedimentation tanks. In the second report the choice for using PHOENICS to set up a mathematical model has been made. Also a start has been made with setting up a model for water movement only. The next report deals with the problems encountered in modelling a varying free-surface flow. Finally in the fourth report further progress in modelling the water flow is presented. In the future the most important parts of these reports will be translated into English.

The present report describes the progress which has been made from July 1993 until July 1994. In chapter 2 a brief description of the flow model is given. Chapter 3 presents the experimental setup in which measurements were carried out. In Chapter 4 the measured data are presented, together with a comparison with computations and analysis. The work done so far to simulate the sedimentation is presented in chapter 5. Finally in chapter 6 the continuation of this research is described.

2 MODELLING THE WATER FLOW

First the flow situation in a storm water sedimentation tank is assumed to be a 2-dimensional one. In that case the flow situation is the following. The water enters the rectangular tank over a weir. Behind this (internal) weir the water is recirculating. Most of the water entering the tank flows along the surface over this recirculation zone. Behind this zone the water is divided more evenly over the full depth. At the other end of the tank water leaves the tank over the second (external) weir. See figure 2.1. It is assumed that the size of the recirculation zone influences the amount of particles which can settle.

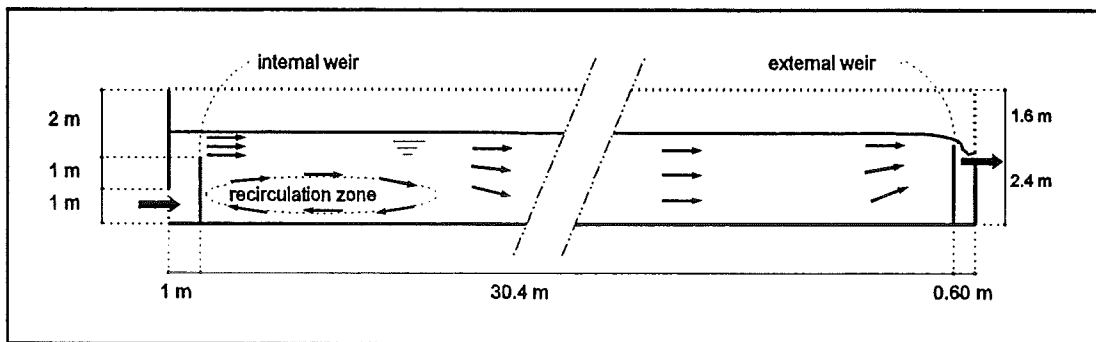


Figure 2.1: 2-dimensional flow situation in tank.

Initially a 2-dimensional model of the flow is set up. In this model the flow domain is divided into many cells. To compute the velocities, in each cell the mass equilibrium equation and the Navier-Stokes equations for the velocities are solved. At the start of a storm the tank is empty. To model the process of filling the movement of the rising water level is to be computed. Also when the tank is filled, the water level varies, because the inflow changes in time. These minor fluctuations of the water level will have to be simulated to take into account correctly the effects of the in time varying inflow. The flow through the tank is a turbulent one. The turbulence is modelled with the generally used k- ϵ model.

For a continuous flow with an almost horizontal water level, the free water surface can be represented by a rigid lid, which means that the top edge of the mathematical model is chosen just at the water surface. A mathematical model of the flow with a rigid lid resulted in an apparently possible flow. However, the length of the computed recirculation zone equals only 6 times the height of the first weir. From observations in a scale model and according to literature [Booij, 1986] this should be between 6 and 8 times this height. The k- ϵ turbulence model used is known to result often in a too short recirculation zone [Booij, 1986].

The next step was the simulation of a free water surface flow. This did cause some problems, but finally the results were satisfying. The filling of a tank can be simulated and the equilibrium situation with a free water surface was studied. It appeared that in a steady state situation the differences in the results of flow computations with and without a free surface are only small. Both with and without a free surface, a boundary condition for ϵ has to be given at the free surface, to prevent too high turbulence there. For a computation without a free surface this boundary condition is at the rigid lid, while for free surface computations it is at the computed surface somewhere in the flow domain. Results of the flow modelling are presented in [Kluck, 1992-b, 1993-a and 1993-b] and in chapter 4.

3 MEASUREMENTS IN A SCALE MODEL

To validate the flow simulations, measurements were carried out from the end of April 1994 until half of June in a scale model of a storm water sedimentation tank in the Hydromechanics Laboratory (Hydraulics department of the Delft University of Technology). The experimental setup has already been presented in [Kluck, 1993-a], but is partly repeated here.

3.1 Experimental setup

The scale model is as presented in figure 3.1. It represents a tank of $30.4 \times 8 \times 2.5$ m³ at a scale of approximately 1:8. The width of the flume is 1.02 m. The other dimensions are given in the figure. The water enters the flume near the bottom on the left. To approximate a 2-dimensional flow, a uniform flow before the first weir is desired, therefore damping material is placed near the inlet. It is emphasized that the initial PHOENICS model of this flow situation is a 2-dimensional one. Consequently the inflow has to be as uniform over the width (2-dimensional) as possible. See also paragraph 4.2.

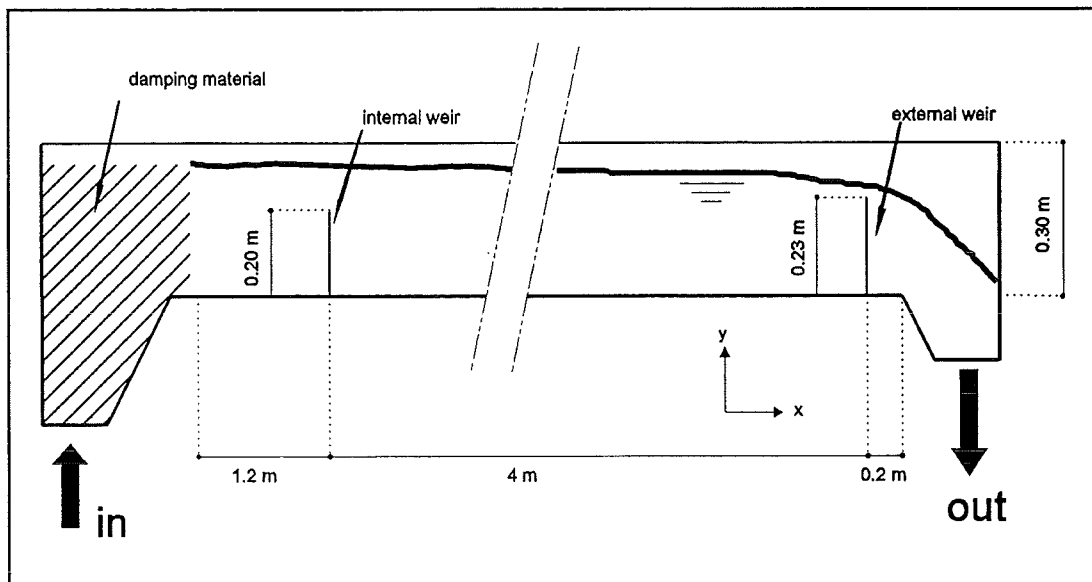


Figure 3.1: Experimental setup.

In this flume 5 flow situations have been investigated. In flow situation 1 and 2 the internal weir and the external weir were 0.20 and 0.23 m high respectively. For the 3rd and 4th situation they were lowered to 0.14 and 0.17 m. The inflow was 30 l/s for situation 1 and 3. For situation 2 and 4 it was 15 l/s. The 5th flow situation is the flow with a diffuser just behind the internal weir, for an inflow of 30 l/s and high weirs (like situation 1).

The weirs consisted of 1.8 cm thick wooden plates. The diffuser was made of bars of 3 cm high and 1.8 cm thick, placed horizontally perpendicular to the main flow direction. Between the bars the gaps were 3 cm high. The first 3 cm from the bottom were closed.

Only steady state flow situations were investigated, because of the available measuring equipment.

The flow situations have been chosen in such a way, that:

- * the Reynolds number is of the same order of magnitude as in the prototype (full scale tank). It is emphasized that the exact value is of no importance ;
- * the Froude number is of the same order of magnitude as in the prototype;
- * the proportion between height of the internal weir and the length of the flume is about the same as in the prototype;
- * the average velocities are not too small for the measuring device.

The flow through the flume is compared with a flow through the prototype with an inflow of 1 m³/s. As can be seen in table 3.1 the flows in the flume do correspond to the flow in the prototype.

Table 3.1: Comparison of flow situations in flume and prototype.

	flow situation in flume				Prototype
	1	2	3	4	
H _i (m)	0.20	0.20	0.14	0.14	2
H _e (m)	0.23	0.23	0.17	0.17	2.4
Q (m ³ /s)	0.030	0.015	0.030	0.015	1.0
h (m)	0.30	0.27	0.24	0.21	2.6
u _{avg} (m/s)	0.10	0.06	0.13	0.07	0.05
L/H _i (-)	20	20	29	29	16
Re (-)	20,000	10,000	20,000	10,000	80,000
Fr (-)	0.06	0.03	0.08	0.05	0.01

An Electromagnetic velocity meter (EMS) was used to measure the velocities in the main flow direction and the vertical direction. From the (turbulent) fluctuations of these velocities in time the turbulent kinetic energy could be estimated. Only one EMS to measure in the horizontal-vertical plane was available. Consequently, to get a complete picture of the flow, for each flow situation measurements had to be carried out at many places one after another. At each location the velocities were recorded for 10 minutes with a sample frequency of 10 Hz. This frequency appeared to be high enough to record the turbulent fluctuations of the velocities. A duration of 10 minutes in fact appeared short to average out the slow flow fluctuations. But with longer durations the measurements would take too long.

Most of the measurements were carried out in the center (at half the width), but to check if the flow was 2-dimensional (see paragraph 4.2) some extra measurements over the cross-section were made. The inflow was measured at 47 cm before the first weir at 5 different heights in the middle and at both sides. The velocity appeared to be higher near the surface. This can be explained by the

shape of the damping material before the first weir, which was thinner near the surface. This unfortunately might influence the flow behind the internal weir. At 5 to 7 different distances of the first weir and at 5 to 7 different heights the velocities in the flume were recorded. In annexes C the results of the measurements are given. The results are presented together with the computational results in paragraph 4.1.

The water level is measured before and after the first weir in order to be able to check the free surface computations, and to choose the location of the rigid lid in the computations without a free surface.

3.2 Effect of distance to the bottom on the measurements

It is assumed that the distance of the probe to the iron bottom influences the measured voltages of the electromagnetic velocity meter. This appeared to be true. In quiescent water, at approximately 80 cm from the first weir, the measured voltages were recorded for 60 seconds at different distances to the bottom. Before the first and after the last of these measurement zero-measurements were carried out to correct for the zero-shift. The results of these measurements are presented in figure 3.2. Although the water was not flowing, voltages were recorded, which have been transferred into velocities. The figure shows clearly that the measured horizontal velocities at the bottom are higher than at some distance from the bottom. The horizontal velocities at 1.5 cm from the bottom (0.5 cm between probe and bottom) are 1.25 cm/s higher than at 10 cm. From 10 to 4 cm the difference is about 0.5 cm/s. From 10 to 7 only 0.1 cm/s. It is concluded that above a depth of 5 cm the interference is negligible.

For the velocity in vertical direction the differences are smaller and therefore negligible.

In an attempt to reduce the effect of the distance to the bottom, first a currency regulator was put between the electricity supply and the experimental setup in order to eliminate any influence of the electricity supply on the measurements. This did not reduce the dependency of the measurements to the distance to the bottom. Also grounding the EMS and the flume (to prevent electrical potential differences) did not make any difference.

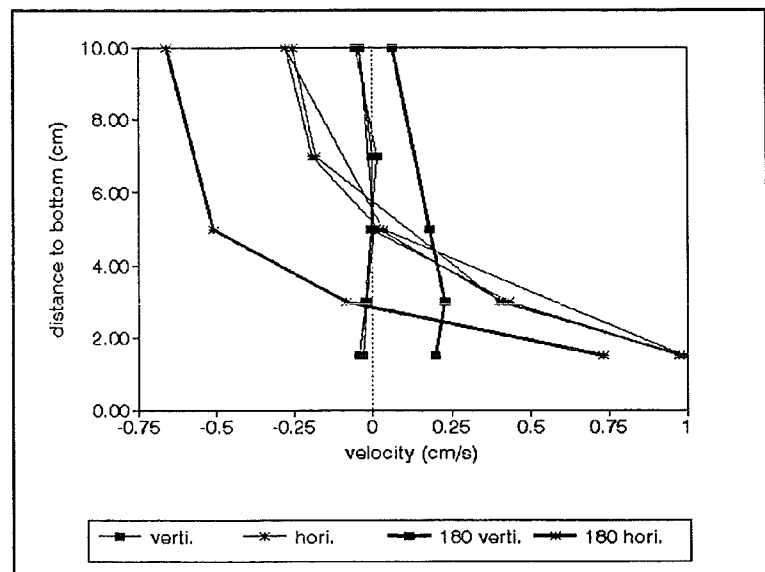


Figure 3.2: Effect of distance to the bottom on the measured horizontal velocity.

A remarkable point is that the measurements with the probe turned for 180° in the horizontal plane show a shift on the horizontal velocity axis between 0.35 and 0.5 cm/s. See figure 3.2. It should be noted that when the probe is turned, the sign of the velocities should be changed (something which has not been done in the figure!). The differences are not large, but for the 5 flow situations all velocities computed out of the measurements with the turned probe might be too high. At least this is the case for quiescent water. With flowing water the differences might be different again.

The measurements for the zero-shift have both been carried out with the probe in the normal position (facing the front of the flume).

3.3 EMS fit

The EMS measures voltages. From these voltages the velocities can be computed with an equation, provided with the EMS, which has been obtained from calibration measurements. The fit through these points is of the form:

$$\text{constant1} \cdot \text{Voltage}^2 + \text{constant2} \cdot |\text{Voltage}| + \text{constant3} = 0$$

Depending on the orientation of the probe in the experimental setup, the velocities will be positive or negative. For small velocities another equation was provided. This equation, based on 6 extra measurements, is of the same form and supposed to be valid for velocities between -3.0 and 3.0 cm/s. See line "Old fit" in figure 3.3. Since the third constant is not equal to zero and the two other terms are both positive this fit will never result in a zero flow.

It was therefore decided to determine a new line which would go through the origin and fit best through the 6 extra measurements and the smallest of the measurements for the higher velocities. The result is presented as the line $x^3 + x^2 + x$ in the figure. This equation is used in all the elaborations of the measurements for voltages smaller than 0.2. For higher voltages the old equation for the high values (given in the figure as E075) is used. For the velocities in the vertical direction in the same way a new fit has been determined.

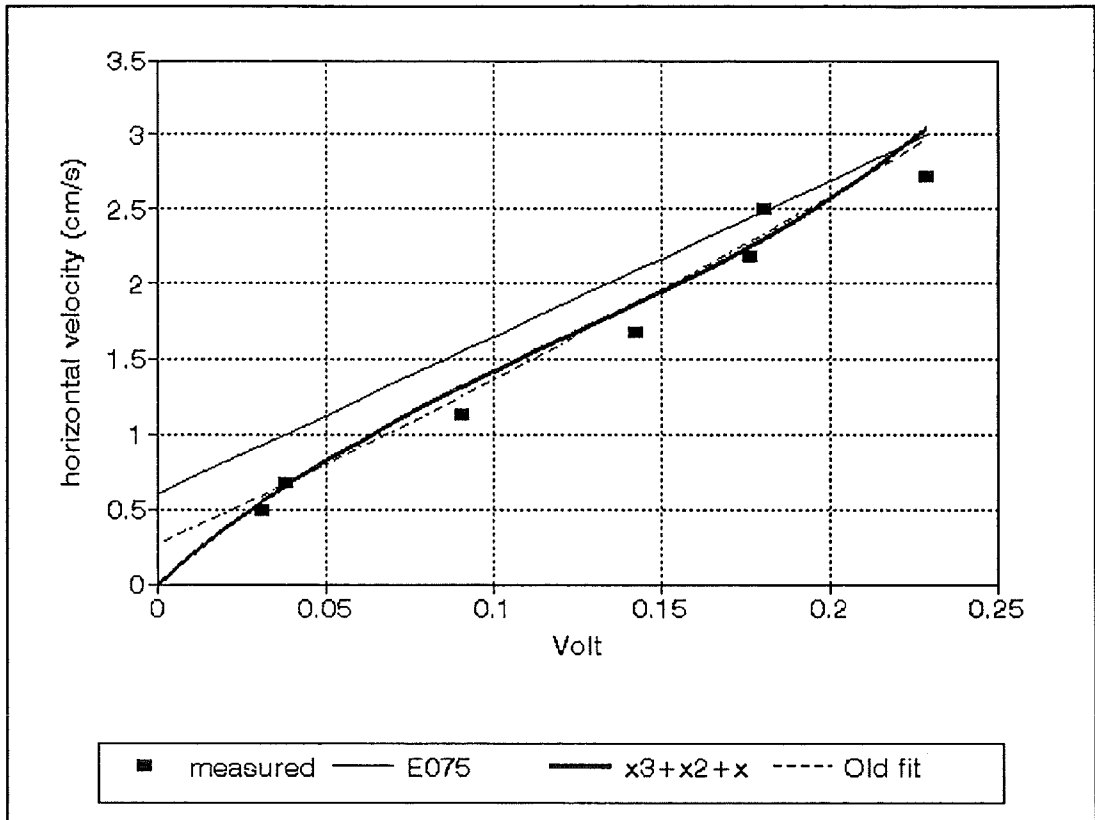


Figure 3.3: EMS fit for horizontal velocities between 0 and 0.22 m/s.

3.4 Zero-measurements

The recording of the EMS-probe in quiescent water (no-flow-situation) is known to change in time [Wit, 1992]. It is assumed that this shift is a linear function of time. To correct for this shift every day before the first measurement the recorded voltages were set to zero. Next, a so called zero-measurement was made: In the flume with quiescent water the measured voltages were recorded for 60 seconds with a frequency of 10 Hz. At the end of the day, after all measurements had been carried out, a second zero-measurement was carried out at the same place. With these two zero-measurements and the registered time of measuring at the different locations each measurement is corrected for the zero-shift.

4 ANALYSIS OF MEASUREMENTS AND COMPUTATIONS

With PHOENICS the 5 measured flow situations in the flume (see table 3.1) were simulated. It is expected that, if the flow in the flume can be simulated well with the mathematical model, also the flow in real tanks can be predicted.

4.1 Comparison of measurements and computations

The preliminary results show that the computations predict the flow reasonably well, but that in the recirculation zone the differences in vertical direction of the horizontal velocities are too small. In figure 4.1, for situation 1 the measured and computed velocities in the mid of the tank are presented at 8 cross sections. In the graph the horizontal velocities are presented relative to the dashed vertical lines which also represent the locations where the measurements were undertaken. 1 m in the graph represents 0.5 m/s.

From the graph it can be deduced that the computed recirculation zone is shorter than the one in the measurements. The computed velocity differences in vertical direction are smaller than the measured differences. This indicates a too high exchange rate of impulse, thus too much diffusion. After the recirculation zone the computations match the measurements reasonably well.

From the measured velocities the k values are calculated. The turbulent kinetic energy is a function of the turbulent fluctuations of the velocities in the x , y and z direction (respectively velocities u , v , and w). The values of u' , v' and w' are equal to the standard deviations of the concerning velocities.

$$k = \frac{1}{2}(u'u' + v'v' + w'w')$$

Because velocities in the z direction (horizontal, perpendicular to the main flow direction) are not available, $w'w'$ has to be estimated. According to [Nezu, 1993]:

$$\frac{u'u'}{2k} = 0.55, \quad \frac{v'v'}{2k} = 0.17, \quad \frac{w'w'}{2k} = 0.28$$

Consequently

$$w'w' = \frac{1}{2.6}(u'u' + v'v')$$

In the same way as the velocities in figure 4.1 the turbulent kinetic energy is given in figure 4.2. In the recirculation zone the computed values of k are far too high. This corresponds to a high turbulence intensity and therefore high turbulent viscosity and diffusion by turbulence. As a result of this the velocities profiles are rather smooth. After the recirculation zone the measurements and the computations correspond better.

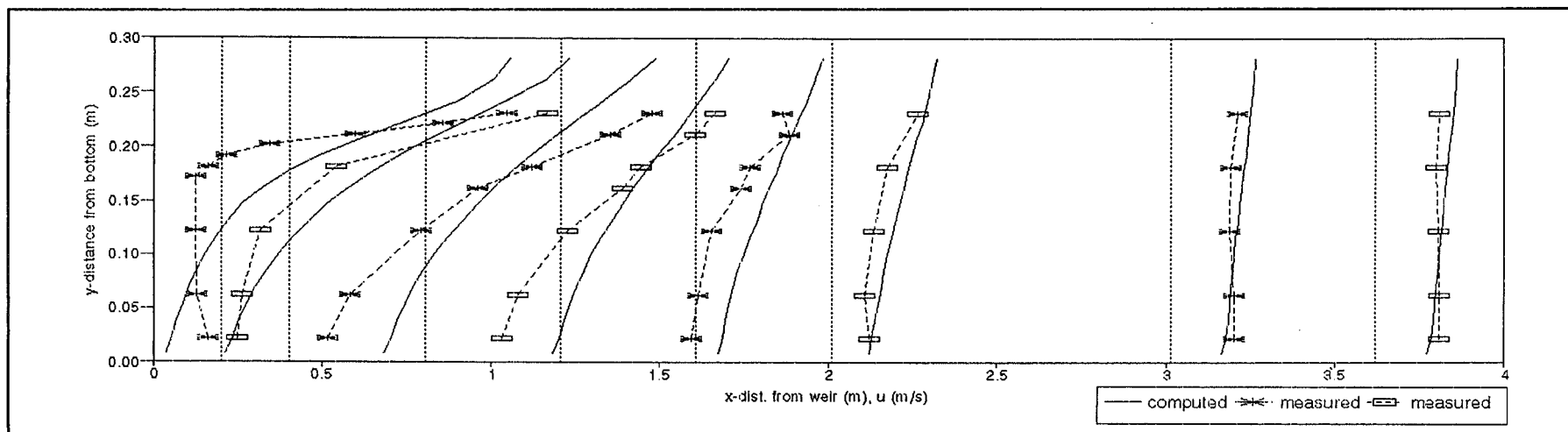


Figure 4.1: Computed versus measured horizontal velocities for situation 1.

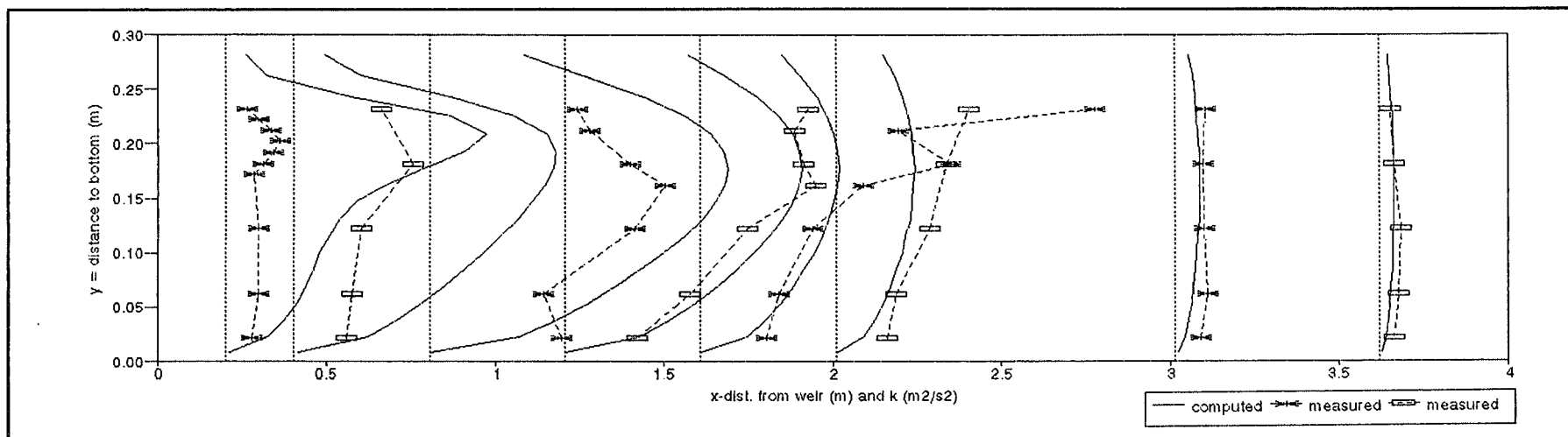


Figure 4.2: Computed versus measured turbulent kinetic energies for situation 1.

For situation 2 the velocities and k values from the measurements and the PHOENICS computations are given in figures 4.3 and 4.4. The figures for the other situations are presented in annexes C. For situation 2 to 4 the computed recirculation zone is again always shorter than the measured one. Like in situation 1 the computed diffusion is too high in the recirculation zone. For situation 5 computations were carried out both with a coarse and with a fine grid. For both computations the differences between the computations and the measurements are large near the diffuser. Downstream of the diffuser the results correspond better.

Computations with and without a free-surface resulted in almost the same flow-situations for the steady state situation. However these final flow situations were reached differently. The computation without a free water surface was carried out as a stationary computation, in which no time period is simulated. For computational reasons the free surface flow computation was carried out as a transient computation, i.e. a computation in which the flow in a time span was simulated. The time span was continued until the final flow situation was reached. Therefore it can be concluded that a time-consuming free-surface simulation is not necessary if only the final steady-state flow situation is of interest.

To reach better resemblance between the measurements and the computations more work has to be done.

It is reported that the k - ϵ turbulence model is amongst possible others responsible for the differences [Booij, 1986]. A modified form of the k - ϵ model (provided in PHOENICS) is used. This modified k - ϵ model is expected to model the turbulence better. A description of the standard and modified k - ϵ model will be given in the following report. In figures 4.3 and 4.4 the measured data of situation 2 is compared to two computations. The thin lines are the results of computations with the standard k - ϵ turbulence model while the bold lines are the results of computations with an modified k - ϵ model. Just behind the first weir in the recirculation zone the velocities computed with the adapted form of the turbulence model are definitely better. The turbulent kinetic energy in that area is also more according to the measurements. However, at the end of the recirculation zone the adapted model leads to worse predictions than the standard. The recirculation zone becomes too long.

Since computations with this modified turbulence model still differ from the measurements more work will have to be done to match the computations to the measurements. It has to be remarked that differences might also be caused by 3-D effects.

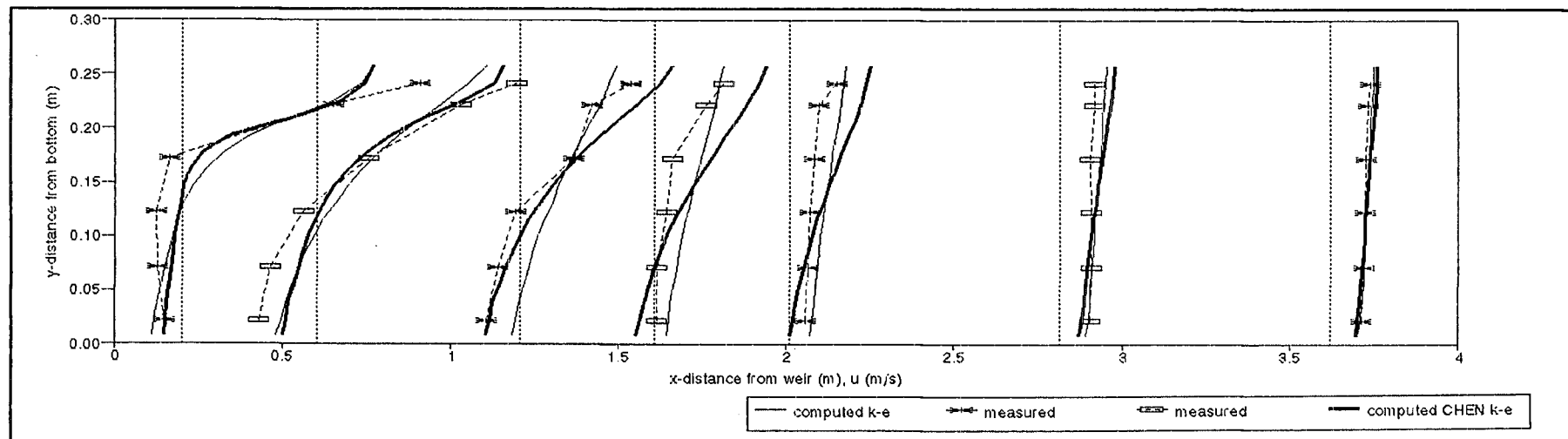


Figure 4.3: Computed versus measured horizontal velocities for situation 2.

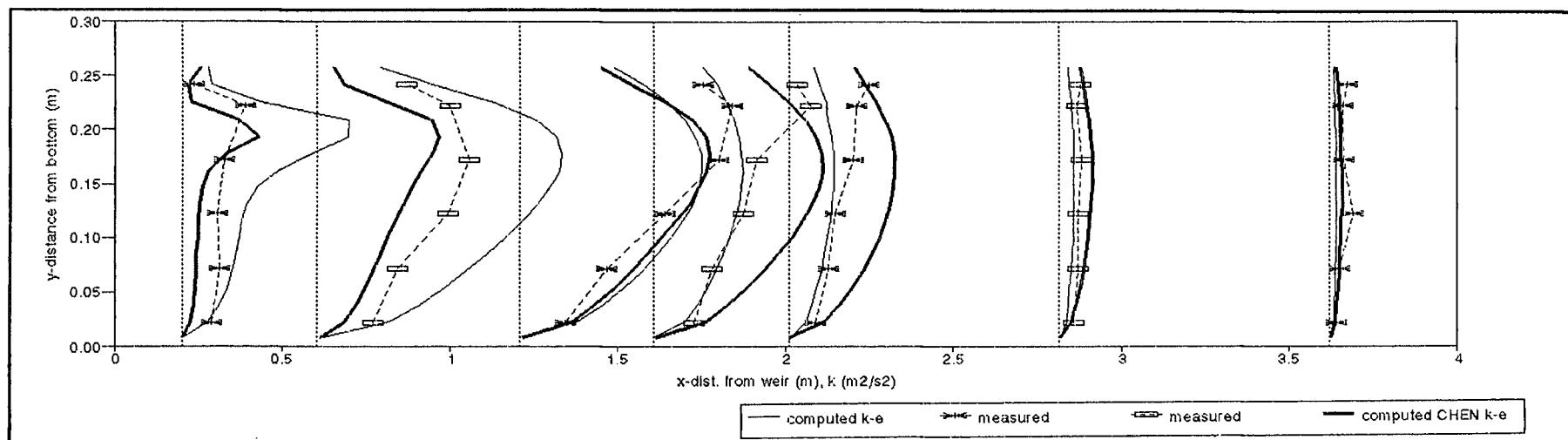


Figure 4.4: Computed versus measured turbulent kinetic energies for situation 2.

4.2 3-D effects

To simplify the mathematical model and to save computational time the flow situations were simulated with a 2-D model. It was hoped for that the flow situation in the flume would be sufficiently 2-dimensional to allow a 2-D simulation. From the measurements it became clear that this is not the case.

As can be seen in figure 4.1 all measured values are smaller than the computed values for $x = 1.6$ m (the fifth cross section from the left). This means that according to the measurements less water is passing through the center-line than according to the computations. The mass balance of the computations is right (exactly 30 l/(s.m) is passing). Near the inflow and the outflow the measured velocities in the mid of a cross section do result in an average flow of 30 l/(s.m). This indicates that at $x = 1.6$ m more water is passing at the sides than in the middle, thus a 3-dimensional flow is present. The measurements in situation 2, 3 and 4 show this same effect.

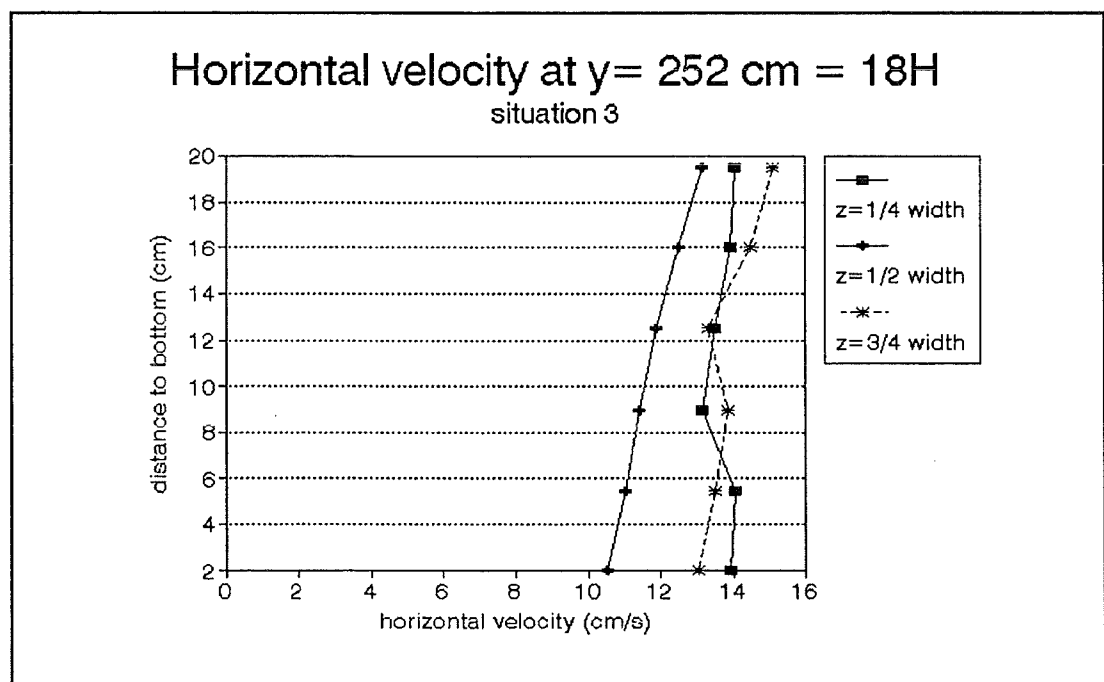


Figure 4.5: Measured horizontal velocities for sit. 3 at 252 cm from the internal weir.

Extra measurements at 1/4 and 3/4 of the width showed that water at the sides is indeed flowing at a higher velocity. In figure 4.5 this is shown for situation 3. The horizontal velocities at 252 cm downstream of the first weir are given on the x axis. On the vertical axis the distance to the bottom is given. It is estimated that the higher velocities at the sides compensate for the smaller velocities in the middle, so that in fact 30 l/s is passing the cross section.

For situation 3 (inflow 30 l/s, low weirs), extensive measurements were planned to check accurately the 3 dimensional flow, but unfortunately the pumps of the experimental setup broke down during these measurements. These series of measurements could therefore not be completed.

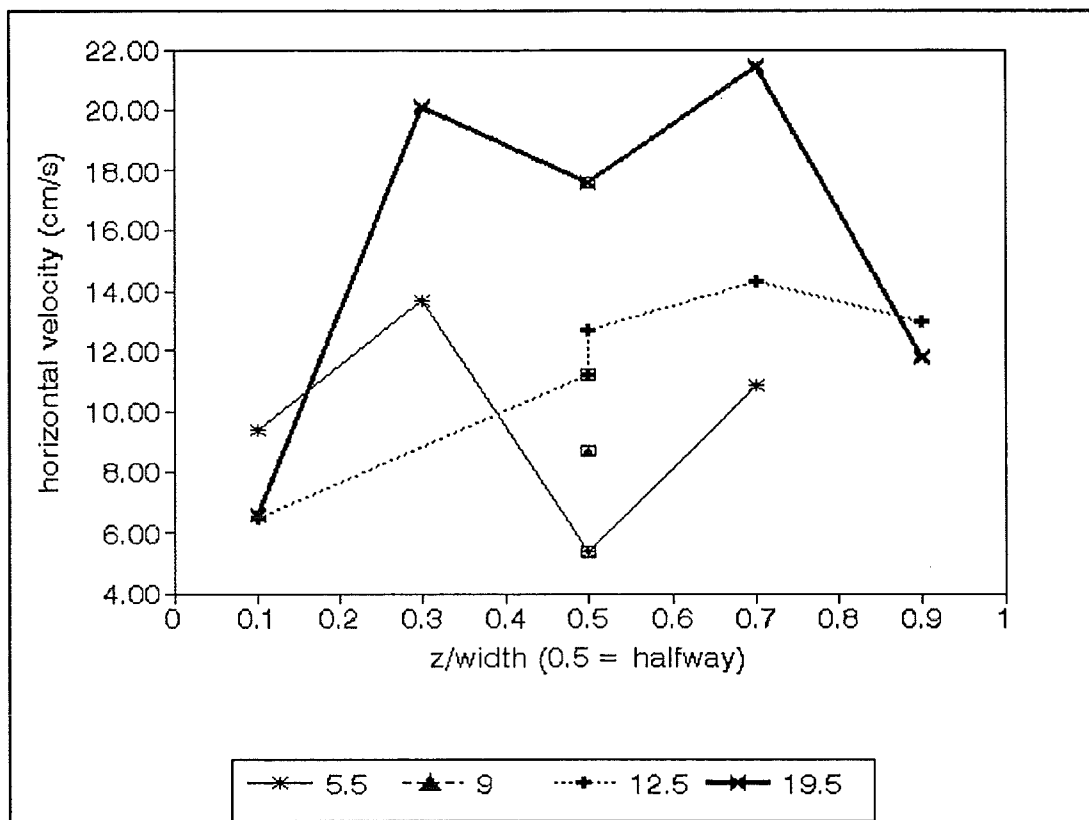


Figure 4.6: Measured horizontal velocities for sit. 3 at $x = 160$ cm.

In figure 4.6 the measured horizontal velocities at 160 cm from the first weir for situation 3 are given on the vertical axis. On the horizontal axis the relative distance to the side wall is given. The figure shows the same 3-dimensional flow as described above.

The 3-dimensional effect could be the result of a non-2-dimensional inflow. To ascertain a 2-dimensional inflow the section before the first weir should have been much longer than it was. Unfortunately such a long flume was not available. To check if the inflow was more or less 2-dimensional, first some tests were carried out with dye in order to visualize the flow. The damping material was adjusted until the flow seemed to be 2-dimensional.

For each flow situation extra measurements were carried out before the internal weir in the middle and at 1/4 and 3/4 of the cross section. These measurements show that for all flow situations the highest velocities occur in the middle. This was expected, because of the wall friction along the sides. The 3-dimensional flow can therefore not be explained with the situation as existed for the first weir.

Another explanation is that the flow situation with friction at the sides, bottom and weirs induces these 3-dimensional effects. To investigate this a 3-dimensional mathematical model has been set up with PHOENICS. Only one half of the width was modelled, as the flow can be expected to be symmetrical. Horizontally perpendicular to the flow half of the tank was divided in 7 cells. Because of the way PHOENICS handles 3-D flow, this larger amount of cells is no problem for the computer. Only the computational time increases considerably. In figure

4.7 the flow vectors in the equilibrium situation are given. The side view of the middle of the tank shows the expected recirculation flow. The flow is clearly 3 dimensional. The vectors at the bottom (seen from above) show a recirculation in the horizontal plane. This recirculation is largest near the bottom.

It is not sure whether this computed flow is correct. This computation has been carried out without the boundary condition for ϵ at the rigid lid and the standard $k-\epsilon$ model has been used for the turbulence. So, more work has to be done before definite conclusions can be drawn.

The 3 cm thick vertically placed bars at the side of the weir, used to fix the weirs in the flume, could also be the cause of the 3-dimensional flow structures. But it is likely that its influence is only small since 3-dimensional flow structures were predicted with the mathematical model in which these bars are not present.

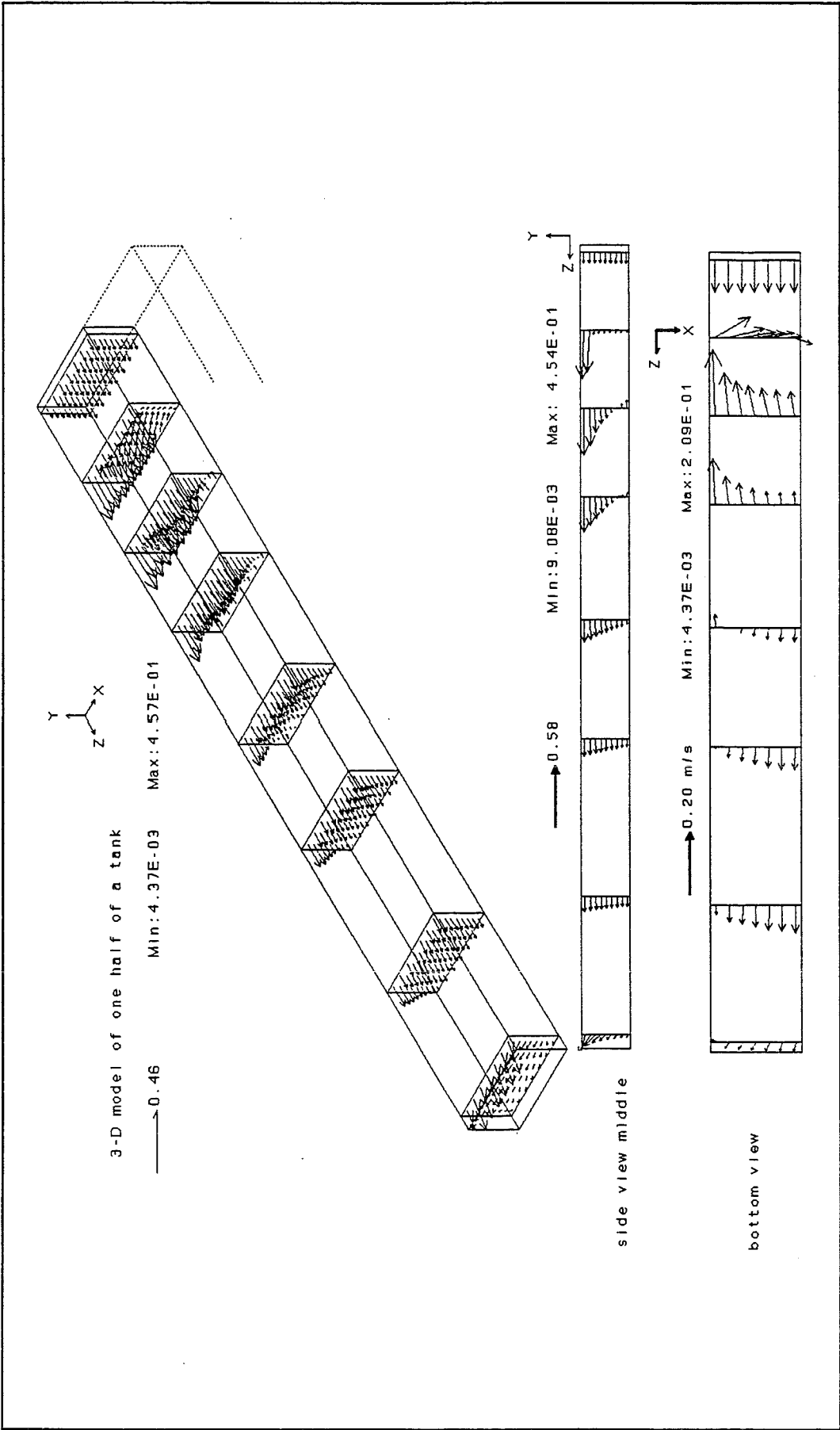


Figure 4.7: Velocity vectors in the 3 dimensional computed flow.

5 SEDIMENTATION

To set up the mathematical model first the particle transport was left out of the model and only the water flow was simulated. The transport of settling particles has to be added to this flow model. Such an extension will have to simulate the following processes. The particles will be transported by the main flow (which is a mixture of water and different types of particles) and will in the same time move downwards relative to the mixture flow due to the gravity. The downward velocity of a particle relative to the mixture flow is called the slip velocity. This slip velocity depends on the particle size and shape, and on the densities of the particle and mixture fluid. Also the concentration of particles may influence this slip velocity, as for high concentrations the settling will be hindered. By (turbulent) diffusion differences in concentrations will be partly levelled out. Depending on the flow situation particles will deposit at the bottom or be entrained into the flow. The particles may be cohesive. Finally, local differences in density may induce density currents.

However in order to set up this part of the model, the particle movement is for the time being simplified as follows:

- * convective transport by the mixture;
- * diffusion;
- * sedimentation with a constant slip velocity, depending on the particle size and density and the fluid density and viscosity;
- * deposition and entrainment.

In the following different models to compute the particle distribution will be described. To simulate the transport of settling particles PHOENICS has been provided with some possibilities. The most suitable of these seems to be the Algebraic Slip Model [*PHOENICS manual*]. The results of computations with this model are promising. However, there are some disadvantages. Therefore it was decided to set up a different model. The results seem possible, but this model is not perfect. Another model is being developed, but still has to be implemented and tested.

5.1 PHOENICS settling model: Algebraic Slip Model

In the PHOENICS manual the following description of Algebraic Slip Model (ASM) is given: "The Algebraic Slip Model computes the distribution of space and time of the concentrations of particles of various sizes and densities, when these move relative to the surrounding fluid under the influence of gravity or other body forces.

It rests on the assumption that the velocity of a dispersed phase relative to the surrounding fluid depends only on local variables, for example:

- * the density difference between the dispersed phase and the medium;
- * the particle size of the dispersed phase;
- * the viscosity of the medium;
- * the local body-force field.

In this model the slip velocities are calculated and added to the mixture velocities to form the particle mass-fluxes crossing cell faces." The fluxes computed, together with the mixture fluxes, are added as sources to the appropriate equilibrium equations. The fully upwind discretisation is used, and the location of

the upwind cells is determined based on the sum of the mixture velocity and the local slip velocity.

With the ASM some computations were made. The results were satisfactory. Deposition was not part of ASM, but appeared easy to implement. Particles which settle at the bottom can be regarded to be out of the flow. The method used was to take out of the fluid a certain percentage of the particles present in the lowest cells. At the preliminary stage of modelling the particle flow, the objective was to investigate the possibilities of modelling this flow. The exact percentage of particles taken out of the lowest cells was not important. In the tests the percentages were varied between 0 and 100%. The amount of deposited particles was recorded. It is also possible to make the amount of deposition dependent on the slip velocity or even on the relation between the horizontal and vertical mixture velocity. The simulations with this model resulted in satisfactory concentration profiles.

The use of the ASM does have some disadvantages. The first is that with the ASM the computed (laminar and turbulent) diffusive particle transport will be negligible for storm water sedimentation tanks. In reality the diffusive turbulent transport will be important. In the ASM the diffusive transport of particles is based on the local density differences of the mixture fluid. Because in storm water sedimentation tanks the density will not vary very much, this transport will be negligible. The density of the mixture is equal to:

$$\rho_m = \frac{1}{\frac{1 - \sum P_t}{\rho_l} + \sum \frac{P_t}{\rho_{sl}}}$$

For example:

One liter of inflowing water is estimated to contain about 20 ml of sludge, consisting of 1% of solid matter, with a density of 2,000 kg/m³. This gives 0.40 kg of particles per m³ of water, or $P_t = 0.04\%$. This means that the inflowing water has a density of 1,000.2 kg/m³. Near the bottom of the tank sediment will concentrate, but the density differences compared to the water density will stay only small and the computed diffusion will be negligible.

Another disadvantage is that this method can not be used (easily) in combination with the free-surface model (attempts to do so failed), because for the ASM and the free surface model conflicting settings are needed.

A last disadvantage of this method is that it is a general method which is written for many different flow situations and for settling (or even flotation) of different types of particles. Because of that the coding is very extensive and contains parts which are not needed to compute the flow in storm water sedimentation tanks.

Like other CFD (Computational Fluid Dynamics) packages PHOENICS is still being developed and new versions appear frequently. In the latest release (version 2.0) the ASM has been changed considerably. The new version of ASM has not yet

been used to compute the particle distribution in storm water sedimentation tanks, but it appears that the disadvantages are still the same.

5.2 Uncoupled convective and settling transport

Because the combination of free-surface flow and ASM appeared not to be possible and because diffusion was not computed in the old version, a new method for the simulation of the sedimentation was developed. The convective transport and the transport due to gravity forces have been uncoupled. Like solubles the particles are subject to the convective and diffusive mixture transport. This kind of transport is standard and expected to be correct within PHOENICS. The fluxes due to gravity transport are added as sources to the equilibrium equation for each kind of particles.

The convective transport is based on the upwind direction of the mixture flow. The sedimentation is always downwards. That means that the discretisation is not fully upwind, simply because to have a fully upwind discretisation, the upwind direction for the particles has to be determined based on the resulting particle velocity, i.e. slip plus mixture velocity. The following example should make this clear:

In case that the mixture velocity is directed upwards and its absolute value is equal to the (downward) slip velocity, the final particle velocity is zero. So no vertical particle transport should be computed. However, with this method upward and downward fluxes are computed. This way extra numerical diffusion (or errors). is introduced.

In fact it is obvious that a settling particle will not be able to settle to the cell below if the mixture velocity is higher than the slip velocity and in the opposite direction. The errors introduced will be smaller when the computational area is divided in more (and thus smaller) cells. How large these errors are and when these errors are small enough has still to be investigated.

The method however is very simple. The following sources IN and OUT are added to the equilibrium equations to compute the particles flowing in and out of cells due to sedimentation.

$$\begin{array}{lll} \text{IN} & = & C_{\text{above}} \cdot v_s \cdot \rho_m \cdot A \quad (\text{kg/s}) \\ \text{OUT} & = & C_p \cdot v_s \cdot \rho_m \cdot A \cdot Sf \quad (\text{kg/s}) \end{array}$$

The sedimentation factor equals 1 if the cell is not at the bottom of the flow domain. At the bottom Sf might be smaller than 1 to adjust the amount of particles sinking through the bottom and leaving the flow (deposition).

To check the working of the model the flow and settling in a long horizontal duct without any obstacles was simulated. This resulted in possible profiles for the velocity and the concentration. At the inflow a logarithmic profile was dictated for the horizontal velocity. At the end of the duct this profile is still almost the same. See figure 5.1. The concentration of particles at the inflow decreases with the distance to the bottom. It was assumed that finally an equilibrium is reached and thus that the sum of deposition and entrainment is zero. Thus $Sf = 0$. It is however not sure if the inflowing amount of particles is the right amount for these flow conditions.

In case of a continuous flow not interrupted by weirs, and thus without an upward flow this seems not to be so important. If the concentration in the lowest row of cells is too high, then because of the sedimentation and absence of an upflow of water, a few cells higher the concentration is hardly influenced. Halfway the duct the equilibrium profile for the particles of 0.04 mm is already nearly reached. The computed concentration-profiles seem to be realistic.

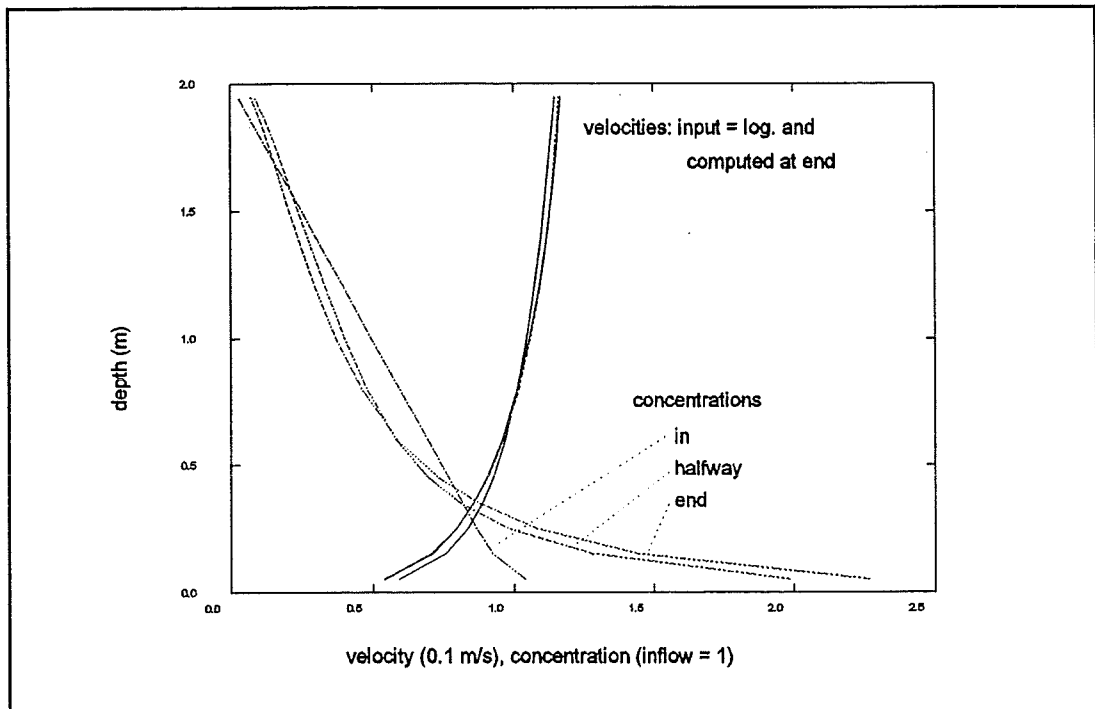


Figure 5.1: Horizontal velocity and concentration in a long duct.

In storm water sedimentation tanks more complicated flow situations will occur. Depending on the flow situations particles will deposit at the bottom or be entrained into the flow. If particles are added to the cells in the lowest row (entrainment), they will be transported to higher cells too, because of convection and diffusion (turbulence). Especially near the weirs, where the flow of liquid moves sediment from (near) the bottom upwards it is important that about the right amount of particles is predicted in the lowest cells, for a good prediction of the distribution of particles. Therefore for the simulation of storm water sedimentation tanks a right boundary condition for deposition and entrainment is important.

An empirical relation between flow characteristics and entrainment was not readily available. To investigate the possibilities of simulating entrainment, the following equation was invented:

$$\text{Entrainment} = \frac{\rho_s A u v_t}{v_s D y} \quad (\text{kg/s})$$

The amount of sediment on the bottom was registered and when no sediment was available no entrainment could occur. The equation might not be the right one, but computations showed that a process of entrainment was simulated. A

literature research related to the modelling of deposition and entrainment is currently being carried out. The result will be reported in one of the following reports.

In a tank with a sloping bottom the particle distribution was computed. The inflow is at the left in figure 5.2. Like before, the water recirculates behind the first weir. At the right the water is leaving the tank over the second weir. The concentration of particles of 0.04 mm is 100% at the inflow. It is stipulated that the exact value of the concentration is not important, since in this method the density of the mixture is independent of the concentrations. From the figure it can be deduced that particles concentrate near the bottom. The lowest concentration is at the water surface near the exit and is only 26% of the inflow. Near the first weir in the recirculation zone water with a high concentration of particles (the highest in the tank, 120 %) is flowing upwards. At the right side the same is happening. Because of this the outflow concentration is about 60% instead of 26%.

To reduce the upflow of particles from the bottom near the second weir, several extra outflow locations were provided on the water surface left of the second weir. Because of this the flow towards the secondary weir became smaller. However the overall effect was negligible. The average outflow concentration over all outflow locations was the same.

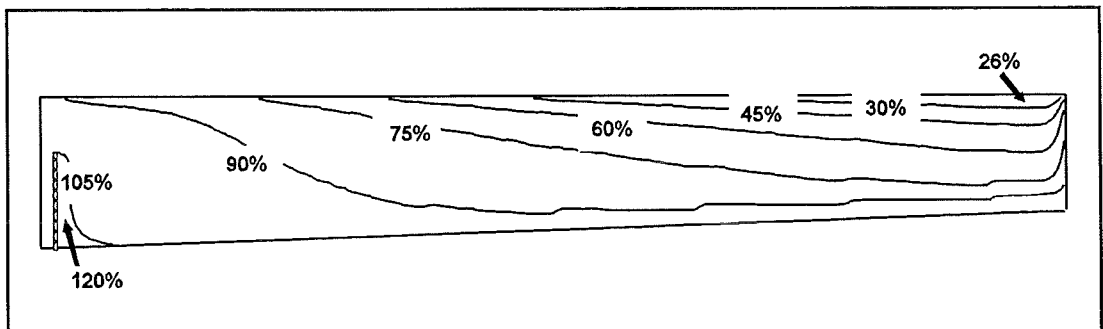


Figure 5.2: Concentration of particles of 0.04 mm in a rectangular tank with sloping bottom; inflow conc.= 1.

The mixture density is taken constant, but can be computed as a function of the particle concentrations. If the local differences in densities are large enough, this results in density currents. Computations with density currents have been carried out. The results have not been calibrated with measurements, but seem not to be unrealistic.

5.3 Uncoupled convective and sediment transport with free-surface flow

The combination of the uncoupled convective and sediment transport method with the computation of a free water surface should work without problems, as in both models no conflicting settings are used. There are however a few problems to solve. In the first place the particles have to be prevented from moving to the air fraction. Without any special attention this will happen because in the free-surface method the water and air fraction are considered as one fluid.

To solve the problem the convective and diffusive fluxes of particles to cells which are filled with air only are set to zero. This way (at least) one other problem is introduced: When the water level behind a weir is lower than the top of the weir (for example behind the first weir during filling), the cells immediately downstream of the weir will be filled with air only. Consequently no particles flow over the weir. For the computation of the water-flow the drop in water level does not seem to be a problem and the results are quite realistic. The water is immediately transported downwards (free-surface method). In an attempt to move the particles right away from the cell above the weir to the first downstream cell with water, the flux of particles (concentration above weir·area·velocity·filling of cell with water) was taken out of the cell above the weir and put in the first filled downstream cell. This nevertheless failed, because the balance of the particles did not add up to zero.

The work on solving this problem has been abandoned because another fully upwind settling method will be set up.

5.4 Another fully upwind settling method

In order to tackle the above mentioned problem an attempt will be made to create another fully upwind method (based on the final particle velocity) to compute the transport of particles. This method should not make the diffusion negligible like it appeared to be in the ASM. Like in the method of uncoupling the convective and the settling transport, convective and diffusive transport is based on the mixture transport in the standard way of PHOENICS. Next a correction for the convective fluxes is made in such a way that the resulting convective flux will be the upwind flux caused by the sum of the mixture and slip velocity. The upward direction will be the y-direction. The gravity forces work in negative y-direction. Only settling (downwards) is accounted for.

This method still has to be implemented and tested. At the moment it is not clear if it is easy to add and subtract the given fluxes. Especially subtracting the right fluxes might be difficult, because sometimes in PHOENICS the computations are done in a slightly different way than expected (or reported).

In the example given above the slip and mixture velocities were assumed to be constant. In the model these will vary in time and space. In the model these will be implemented in the right way. Also the density will vary in time and space.

5.5 Particle size

In sewage particles of different sizes are present. Which sizes enter the tank depends, amongst others, on the following factors:

- * The way the tank is connected to the sewer system. If the flow in the sewer is reasonable quiet only the lighter particles will enter the tank. For on-line tanks all particles will enter;
- * The slope of the sewer system;
- * The level of maintenance and cleaning of the system;
- * The soil-type.

In the first computations the diameters of the particles were varied between 0.04 and 0.08 mm. Particles of 0.04 mm are classified as coarse silt or very fine sand. It is assumed that the pollution is connected to the silt. Particles of 0.080 mm are classified as sand. For small sedimentation Reynolds numbers¹ the slip velocities for round particles is estimated with the Stokes equation:

$$v_s = \frac{gd^2 \rho_s - \rho_m}{18\nu \rho_f}$$

For particles of 0.04 and 0.08 mm this results in 0.0014 and 0.0057 m/s respectively.

More research has to be done to investigate what kind of particles enter storm water sedimentation tanks and which particles have to be retained in the tank. To reduce the pollution sufficiently the flow conditions will have to be such that the small particles with small settling velocities settle.

5.6 Alternative numerical differential schemes

Instead of the fully upwind scheme, different schemes can be used for scalar variables (like concentration) in PHOENICS. In some flow situations this leads to more realistic results than the fully upwind method, because the numerical diffusion will be smaller. On the other hand it will cost some extra computational time.

The scheme known under the name QUICKEST [CHAM, 1994], [Stelling and Booij, 1994] is one of the options.

It is however uncertain how these methods are to be combined with the sedimentation methods of the author.

⁽¹⁾Which is different from the Reynolds number for the flow. The Reynolds number of the sedimentation is $\frac{Re = v_s d}{\nu}$

6 CONTINUATION OF THE RESEARCH

In the coming period the flow model will be adjusted, to bring results of the computations in accordance with the measurements. Since it would be very time consuming to measure the 3-dimensional flow in the experimental setup extensively, it is proposed to calibrate the flow model both by means of the collected measurements and measurements of a turbulent flow in a backward facing step by Tropea [Tropea, 1982].

Computations with 3-dimensional models will be needed to calibrate the flow model to the own measurements. To save computational time the flow will be simulated 2-dimensionally when possible. It is expected that the use of a modified turbulence model will be beneficial. The different turbulence models provided in PHOENICS, will be studied and tested, and hopefully one will yield satisfactory results.

The flow modelling of the flow through the diffuser (as measured in the experimental setup: Situation 5) demands extra attention. It might be advantageous to apply a finer grid only round the diffuser. The possibilities of applying a fine grid only locally (fine grid embedment) have to be investigated.

Next to the calibration of the flow model, the coming period time will be spent on incorporating the sedimentation process. The new method as described in paragraph 5.4 will be implemented and tested. In order to modify the computed convective fluxes in the right way it will be necessary to investigate in what way exactly a concentration is defined

The next report, covering these subjects is expected for December 1994. The further continuation of this research will contain the following:

With the validated flow model the filling of a tank will be investigated in more detail as done in [Kluck, 1993-a]. Evaluating different shapes of tanks will not be carried out extensively until the sedimentation is part of the model. Only the possibilities of the model to compute the flow in different flow situations will be tested.

Measure data to validate the sedimentation method will be collected, preferably from literature. The municipality of Amsterdam is going to carry out measurements in a storm water sedimentation tank. Probably the results can be used to validate the model. A literature research on the modelling of deposition and entrainment will be carried out. More work has to be done to investigate what kind of particles enter storm water sedimentation tanks and which particles have to be retained in the tank.

As part of the setting up and testing of the mathematical model some combinations of features or options of PHOENICS have to be tested. For example, computational grids based on a polar coordinates (round tank) or body fitted coordinates (odd shapes in tank), instead of Cartesian coordinates, have been used with good results. For some applications however, it has to be checked if they perform correctly with these kinds of grids.

With the final functioning complete model (flow and sedimentation) the working of different shapes of tanks can be examined for time varying inflows. If the computational time to simulate one storm through a tank can be kept small enough, it will be possible to evaluate different designs for a range of storms.

ANNEXES A: REFERENCES

Booij R., 1986, *Turbulentie in de waterloopkunde*, lecture notes b82, TUD, Delft.

CHAM, 1994, *POLIS: PHOENICS on line information system*, part of PHOENICS version 2.0, 1994.

Kluck, J., 1992-a, *Onderzoek aan bergbezinktanks: Stand van zaken*, TUD, Delft.

Kluck J., 1992-b, *Een mathematisch model voor het hydraulische gedrag van bergbezinktanks*, TUD, Delft.

Kluck, J., 1993-a, *Het modelleren van een vrij wateroppervlak in bergbezinktanks*, TUD, Delft.

Kluck, J., 1993-b, *Modellering van de waterbeweging in bergbezinktanks met PHOENICS* TUD, Delft.

Stelling G.S. and Booij N., 1994, *Computational modelling in open channel hydraulics*, lecture notes B84, TUD, Delft.

Tropea C., 1982, *Die turbulente Stufenströmung in Flachkanälen und offenen Gerinnen*.

P.J. de Wit, 1992, *Instruments used in the research on cohesive sediments*, TUD, report no. 8-92, Delft.

ANNEXES B: LIST OF SYMBOLS

A	= bottom surface of cell;
b	= width (= 1.02 m in the flume, 8 m in the prototype);
C_p	= concentration in cell P;
C_{above}	= concentration in cell above cell P;
d	= diameter;
Dy	= cell height;
Fr	= Froude number = $u_{avg}/\sqrt{g \cdot h}$;
g	= gravity acceleration;
h	= water depth;
H	= height internal weir;
H_i	= height internal weir;
H_e	= height external weir;
k	= turbulent kinetic energy;
L	= length (= 4 m in the flume, 30.4 m in the prototype);
Pt_i	= mass percentage of particle i;
Q	= inflow;
R	= $b \cdot h / (b + 2h)$;
Re	= Reynolds number = $u_{avg} \cdot R / \nu$;
Sf	= sedimentation factor;
u	= local horizontal velocity in main flow direction;
u_{avg}	= average velocity;
v	= local vertical velocity;
v_s	= slip velocity;
w	= local horizontal velocity perpendicular to main flow direction;
x	= distance from first weir;
y	= distance from bottom;
z	= distance from front side of experimental setup;
ρ_l	= density of the liquid;
ρ_m	= density of the mixture;
ρ_s	= density solids;
ρ_{si}	= density of particle i;
ν	= viscosity.
ν_s	= turbulent viscosity.

ANNEXES C: MEASUREMENTS

ACKNOWLEDGEMENT

I like to thank the French student Stephanie Jandard of the Ecole National des PONTS et CHAUSSEES who carried out the measurements in the experimental setup during May and the first half of June 1994.

EXPERIMENTAL SETUP

General

The tank is 407.8 cm long and 102.8 cm wide. The weirs are 1.8 cm thick.

X: vertical direction

Y: downstream direction

Z: cross-stream

- Situation 1:** Height internal weir = 20.1 cm;
Height external weir = 23.4 cm;
 $Q = 30$ l/s;
Water level before the internal weir at $y = 30.1$ cm;
Water level after the internal weir at $y = 29.1$ cm.
- Situation 2:** Height internal weir = 20.1 cm;
Height external weir = 23.4 cm;
 $Q = 15$ l/s;
Water level before the internal weir at $y = 27.2$ cm;
Water level after the internal weir at $y = 26.5$ cm.
- Situation 3:** Height internal weir = 14.0 cm;
Height external weir = 17.0 cm;
 $Q = 30$ l/s;
Water level before the internal weir at $y = 24.5$ cm;
Water level after the internal weir at $y = 22.7$ cm.
- Situation 4:** Height internal weir = 14.0 cm;
Height external weir = 17.0 cm;
 $Q = 15$ l/s;
Water level before the internal weir at $y = 21.2$ cm;
Water level after the internal weir at $y = 20.6$ cm.
- Situation 5:** Height internal weir = 20.1 cm;
Height external weir = 23.4 cm;
 $Q = 30$ l/s;
Water level before the internal weir at $y = 30.3$ cm;
Water level between diffusor and internal weir at $y = 29.2$ cm;
Water level after the diffusor weir at $y = 29.1$ cm.
The diffusor is at 20 cm downstream of the internal weir. It consists of 5 horizontally (perpendicular to the main flow direction) placed bars of 3 cm high and 1.8 cm thick. The gaps between the bars are 3 cm high. The first bar is at the bottom.

Situation 1, inflow $x = -47$ cm

horizontal velocities in cm/s						
z/width:	0.25		0.5		0.75	
y cm	Avg	Std	Avg	Std	Avg	Std
3.2	12.5	1.40	13.5	0.69	13.1	0.60
8.2	9.0	1.55	10.7	1.24	9.9	1.12
13.2	5.4	1.20	5.7	1.01	5.1	0.75
18.2	4.4	0.53	4.4	0.46	4.6	0.47
23.2	7.8	1.16	9.5	1.37	8.9	0.98
28.2	14.4	1.17	19.0	1.19	17.5	1.21
vertical velocities in cm/s						
z/width:	0.25		0.5		0.75	
y cm	Avg	Std	Avg	Std	Avg	Std
3.2	0.3	0.77	0.4	0.48	0.9	0.38
8.2	-0.5	1.23	-0.0	0.84	0.4	0.72
13.2	-0.7	0.88	-0.5	0.79	-0.3	0.66
18.2	-0.8	0.52	-0.9	0.51	-0.7	0.42
23.2	-1.1	0.78	-1.2	0.77	-1.0	0.65
28.2	-1.3	0.73	-1.4	0.55	-1.1	0.57

Situation 1, flow $z = 1/2$ width

horizontal velocities in cm/s																
x/H:	1		2		4		6		8		10		15		18	
y cm	Avg	Std	Avg	Std	Avg	Std	Avg	Std	Avg	Std	Avg	Std	Avg	Std	Avg	Std
2.2	-2.0	3.28	-7.7	4.74	-14.4	7.88	-8.7	4.80	-0.5	4.35	5.6	4.23	9.5	3.21	9.7	2.31
6.2	-3.5	3.49	-7.0	4.72	-11.2	5.81	-6.2	5.95	0.4	4.34	4.8	4.08	9.5	3.21	9.6	2.16
12.2	-3.7	3.42	-4.3	4.91	-0.7	8.39	0.9	7.68	2.4	5.72	6.2	5.34	8.8	2.71	9.5	2.31
16.2	-	-	-	-	7.9	9.26	9.2	9.60	6.7	7.45	-	-	-	-	-	-
17.2	-3.7	2.98	-	-	-	-	-	-	-	-	-	-	-	-	-	-
18.2	-1.9	3.52	7.0	6.09	15.8	8.49	12.0	9.36	8.0	8.88	8.3	6.13	8.9	2.72	9.1	1.98
19.2	0.7	3.81	-	-	-	-	-	-	-	-	-	-	-	-	-	-
20.2	7.2	3.99	-	-	-	-	-	-	-	-	-	-	-	-	-	-
21.2	19.7	3.84	-	-	27.6	7.51	20.0	9.43	13.7	8.67	-	-	-	-	-	-
22.2	32.8	3.21	-	-	-	-	-	-	-	-	-	-	-	-	-	-
23.2	42.4	2.64	38.3	5.38	33.7	7.38	23.0	9.90	12.8	11.48	12.9	7.25	9.8	3.14	9.6	1.77
vertical velocities in cm/s																
y cm	Avg	Std	Avg	Std	Avg	Std	Avg	Std	Avg	Std	Avg	Std	Avg	Std	Avg	Std
2.2	1.4	1.35	2.0	1.58	1.1	0.91	1.4	3.37	1.3	3.52	1.3	2.48	0.5	1.58	0.4	1.32
6.2	1.3	1.95	2.3	2.35	0.9	4.57	0.6	4.89	0.7	4.32	0.9	3.49	-0.1	2.36	0.1	2.16
12.2	1.9	1.93	2.5	2.88	-0.5	5.21	-1.2	5.27	-0.2	4.60	-0.1	4.06	-0.2	2.58	-0.1	2.31
16.2	-	-	-	-	-1.6	5.15	-2.5	5.22	-0.9	4.73	-	-	-	-	-	-
17.2	2.1	2.20	-	-	-	-	-	-	-	-	-	-	-	-	-	-
18.2	1.6	2.33	0.0	4.44	-2.2	4.81	-2.4	5.12	-0.9	6.37	-0.4	3.90	-0.3	2.47	-0.2	1.93
19.2	1.0	2.87	-	-	-	-	-	-	-	-	-	-	-	-	-	-
20.2	-0.6	3.12	-	-	-	-	-	-	-	-	-	-	-	-	-	-
21.2	-2.7	2.60	-	-	-2.7	4.41	-2.3	4.52	-1.4	4.30	-	-	-	-	-	-
22.2	-3.9	2.27	-	-	-	-	-	-	-	-	-	-	-	-	-	-
23.2	-2.2	1.89	-2.5	3.65	-2.6	3.97	-2.3	4.21	-1.1	7.45	-0.9	3.23	-0.5	2.23	-0.3	1.77

Situation 2, inflow x = -47 cm

horizontal velocities in cm/s							
z/width:	0.25		0.5		0.75		
y cm	Avg	Std	Avg	Std	Avg	Std	
2.2	-	-	7.2	0.40	7.1	0.37	
3.2	7.5	0.86	-	-	-	-	
7.2	5.8	0.98	6.4	0.63	5.5	0.63	
12.2	3.5	0.56	3.7	0.61	3.1	0.46	
17.2	3.4	0.36	3.0	0.40	2.9	0.42	
22.2	6.2	0.59	6.0	0.62	6.0	0.61	
25.4	8.9	0.57	8.2	0.57	7.3	0.51	
vertical velocities in cm/s							
z/width:	0.25		0.5		0.75		
y cm	Avg	Std	Avg	Std	Avg	Std	
2.2	-	-	0.4	0.36	0.3	0.34	
3.2	0.1	0.60	-	-	-	-	
7.2	-0.3	0.72	-0.4	0.51	-0.6	1.37	
12.2	-0.4	0.49	-0.7	0.53	-0.8	0.38	
17.2	-0.6	0.37	-1.0	0.33	-1.1	0.34	
22.2	-0.9	0.49	-1.2	0.38	-1.3	0.36	
25.4	-1.2	0.35	-1.5	0.36	-1.3	0.35	

Situation 2, x = 60 cm = 3H

horizontal velocities in cm/s					
z/width:	0.25		0.75		
y cm	Avg	Std	Avg	Std	
4.2	-6.3	3.08	6.5	3.40	
13.2	2.0	4.21	1.8	4.36	
22.2	23.1	4.12	24.3	4.22	
vertical velocities in cm/s					
z/width:	0.25		0.75		
y cm	Avg	Std	Avg	Std	
4.2	1.6	2.04	-0.9	2.62	
13.2	-2.9	2.85	0.2	2.87	
22.2	-3.8	2.75	-1.8	2.54	

Situation 2, x = 280 cm = 14H

horizontal velocities in cm/s					
z/width:	0.25		0.75		
y cm	Avg	Std	Avg	Std	
4.2	5.8	1.80	4.9	2.18	
13.2	5.7	1.88	5.0	1.83	
22.2	6.1	2.30	6.0	2.23	
vertical velocities in cm/s					
z/width:	0.25		0.75		
y cm	Avg	Std	Avg	Std	
4.2	0.2	1.83	-3.3	1.12	
13.2	-2.1	1.59	-1.0	1.62	
22.2	-2.3	2.19	1.5	1.56	

Situation 2, flow $z = 1/2$ width

horizontal velocities in cm/s														
x/H:	1		3		6		8		10		14		18	
y cm	Avg	Std	Avg	Std	Avg	Std	Avg	Std	Avg	Std	Avg	Std	Avg	Std
2.2	-2.6	2.52	-8.7	3.40	-5.0	2.71	0.3	2.62	2.4	2.26	4.6	1.77	4.8	1.22
7.2	-3.6	2.71	-7.1	3.69	-3.3	3.62	0.3	2.93	2.8	2.42	4.8	1.80	5.1	1.32
12.2	-3.7	2.61	-2.0	4.78	-0.7	4.91	1.9	3.80	3.1	2.56	4.8	1.78	5.2	1.15
17.2	-1.7	2.66	7.6	5.13	8.1	6.01	2.6	4.19	3.6	3.34	4.6	1.97	5.5	1.46
22.2	22.5	3.14	21.3	4.85	10.7	6.50	7.7	5.63	4.5	3.56	5.3	1.77	5.8	1.32
25.4	35.5	1.21	29.7	4.09	16.5	6.28	10.3	5.54	7.0	4.13	5.4	2.12	6.2	1.65
vertical velocities in cm/s														
x/H:	1		3		6		8		10		14		18	
y cm	Avg	Std	Avg	Std	Avg	Std	Avg	Std	Avg	Std	Avg	Std	Avg	Std
2.2	0.6	0.96	1.0	1.36	0.9	1.92	1.2	1.65	1.0	1.18	0.5	0.78	0.6	0.50
7.2	0.4	1.26	0.6	2.33	-0.6	2.81	0.7	2.33	0.3	1.90	-0.1	1.23	-0.1	0.87
12.2	0.7	1.31	-0.2	2.87	-0.7	3.27	-0.3	2.65	-0.3	2.09	-0.2	1.33	-5.1	2.14
17.2	0.2	1.74	-1.2	3.18	-2.3	3.39	-0.4	2.64	-0.2	2.03	-0.2	1.33	-3.5	1.22
22.2	-2.5	2.29	-1.6	2.88	-1.1	2.95	-0.5	2.35	-0.5	1.91	-0.4	1.16	-2.5	1.19
25.4	-4.3	1.05	-3.2	2.12	-1.1	2.11	-0.5	1.86	-0.7	1.39	-0.5	0.90	-1.1	1.35

Situation 3, inflow $x = -47$ cm

horizontal velocities in cm/s							
z/width:	0.25		0.5		0.75		
y cm	Avg	Std	Avg	Std	Avg	Std	
2	17.0	1.72	18.9	0.81	18.2	0.74	
6	13.5	2.02	15.2	1.52	13.9	1.38	
10	9.3	1.74	9.6	1.30	9.2	1.02	
14	7.2	0.73	7.9	0.53	7.4	0.44	
18	9.0	0.66	10.2	0.61	10.2	0.65	
21	11.7	0.76	14.3	0.61	13.2	0.55	
vertical velocities in cm/s							
z/width:	0.25		0.5		0.75		
y cm	Avg	Std	Avg	Std	Avg	Std	
2	-0.1	1.03	0.3	0.56	0.2	0.52	
6	-0.4	1.35	-0.2	0.97	-0.2	0.86	
10	-0.6	1.15	-0.6	1.00	-0.7	0.83	
14	-0.8	0.70	-1.1	0.55	-1.3	0.45	
18	-1.1	0.43	-1.0	0.35	-1.4	0.34	
21	-1.4	0.40	-1.3	0.33	-1.5	0.27	

Situation 3, flow $z = 1/2$ width

horizontal velocities in cm/s														
x/H:	1		1.4		4.3		8.6		11.4		18		27	
y cm	Avg	Std	Avg	Std	Avg	Std	Avg	Std	Avg	Std	Avg	Std	Avg	Std
2.0	-2.1	4.55	-6.1	5.28	-15.9	5.65	0.7	4.89	6.0	3.73	10.5	2.94	11.5	1.95
5.5	-3.9	5.23	-5.9	4.97	-8.7	7.22	2.5	5.48	6.5	4.13	11.0	2.84	12.3	1.79
9.0	-4.5	4.36	-4.9	4.91	-0.2	8.37	6.5	7.16	8.5	4.81	11.4	3.05	12.7	1.65
12.5	-3.4	4.06	1.9	5.06	12.2	9.05	10.2	8.07	11.1	5.78	11.9	3.38	13.3	1.76
16.0	24.2	4.23	30.7	5.21	27.8	8.46	16.0	8.78	14.1	6.66	12.5	3.82	13.7	1.70
19.5	56.1	1.27	53.4	1.52	44.1	5.77	22.7	8.89	16.2	7.13	13.2	3.93	14.2	1.94
vertical velocities in cm/s														
x/H:	1		1.4		4.3		8.6		11.4		18		27	
y cm	Avg	Std	Avg	Std	Avg	Std	Avg	Std	Avg	Std	Avg	Std	Avg	Std
2.0	0.7	1.25	0.6	1.58	0.2	3.18	-0.3	3.11	0.3	2.31	0.2	1.51	0.6	1.04
5.5	0.5	2.00	1.2	2.21	-1.5	4.81	-1.6	4.19	-0.1	3.08	-0.0	2.11	0.2	1.17
9.0	1.0	2.28	1.3	2.61	-2.4	5.66	-2.0	4.86	-0.3	3.84	-0.1	2.32	0.1	1.30
12.5	0.9	2.29	-0.1	3.35	-4.2	4.97	-2.5	4.74	-1.3	3.97	-0.4	2.68	-0.2	1.40
16.0	-2.9	2.26	-2.6	3.09	-4.1	4.32	-2.8	4.54	-1.7	3.61	-0.7	2.39	-0.3	1.30
19.5	-0.2	1.36	-0.6	1.42	-4.9	2.70	-2.9	3.57	-1.9	2.95	-0.8	1.89	-0.6	1.09

Situation 3, $x = 42 \text{ cm} = 3H$

horizontal velocities in cm/s							
z/width:	0.25		0.5		0.75		
y cm	Avg	Std	Avg	Std	Avg	Std	
3.0	-11.7	5.50	-13.7	5.32	-12.3	5.38	
8.5	-1.5	6.83	-5.0	6.81	-2.7	7.08	
14.0	21.1	7.32	17.8	8.07	24.5	8.01	
19.5	49.7	3.79	49.1	4.33	52.8	3.32	
vertical velocities in cm/s							
z/width:	0.25		0.5		0.75		
y cm	Avg	Std	Avg	Avg	Avg	Avg	
3.0	1.5	3.17	1.2	2.71	0.5	2.99	
8.5	-0.1	4.51	0.4	4.46	-0.4	4.45	
14.0	-3.1	4.51	-3.1	4.59	-3.0	4.14	
19.5	-5.5	2.30	-4.1	2.36	-4.1	1.95	

Situation 3, $x = 252 \text{ cm} = 18H$

horizontal velocities in cm/s					
z/width:	0.25		0.75		
y cm	Avg	Std	Avg	Std	
2.0	13.9	3.78	13.1	3.74	
5.5	14.1	3.39	13.5	3.46	
9.0	13.2	3.44	13.9	3.23	
12.5	13.5	3.54	13.3	3.41	
16.0	13.9	3.51	14.5	3.76	
19.5	14.1	3.93	15.1	3.72	
vertical velocities in cm/s					
z/width:	0.25		0.75		
y cm	Avg	Std	Avg	Std	
2.0	0.1	1.73	0.3	1.50	
5.5	-0.8	2.34	-0.7	2.21	
9.0	-1.1	2.51	-1.0	2.55	
12.5	-1.2	2.65	-0.9	2.46	
16.0	-1.2	2.32	-0.9	2.37	
19.5	-1.1	1.85	-0.8	1.89	

Situation 4, inflow $x = -47$ cm

horizontal velocities in cm/s							
z/width:	0.25		0.5		0.7		
y cm	Avg	Std	Avg	Std	Avg	Std	
2.5	10.5	0.91	10.2	0.46	10.0	0.46	
5.5	9.5	1.13	9.4	0.71	9.0	0.66	
8.5	7.2	1.19	7.3	0.89	6.6	0.72	
11.5	5.6	0.96	5.5	0.72	4.7	0.44	
14.5	4.6	0.34	5.2	0.41	5.2	0.40	
17.5	5.4	0.38	6.0	0.39	7.1	0.40	
vertical velocities in cm/s							
z/width:	0.25		0.5		0.7		
y cm	Avg	Std	Avg	Std	Avg	Std	
2.5	-0.1	0.65	0.2	0.42	0.3	0.38	
5.5	-0.5	0.81	-0.4	0.64	-0.6	0.53	
8.5	-0.7	0.89	-0.6	0.76	-0.8	0.59	
11.5	-0.8	0.71	-0.8	0.67	-1.1	0.46	
14.5	-1.1	0.45	-1.1	0.49	-1.3	0.32	
17.5	-1.2	0.29	-1.1	0.27	-1.3	0.28	

Situation 4, flow $z = 1/2$ width

horizontal velocities in cm/s																	
x/H:	1		3		6		8		10		14		18		27		
y cm	Avg	Std	Avg	Std	Avg	Std	Avg	Std	Avg	Std	Avg	Std	Avg	Std	Avg	Std	
3.0	2.7	3.24	-8.9	3.95	-5.6	3.58	-0.3	3.16	2.0	2.57	4.8	2.22	5.5	1.52	6.4	0.91	
6.0	3.1	3.08	-6.7	4.10	-3.4	4.65	1.3	4.12	2.0	2.65	5.2	1.97	5.9	1.59	6.9	0.96	
9.0	2.5	2.90	-2.0	4.74	0.6	5.79	2.7	4.73	4.5	4.02	5.1	2.41	5.7	1.67	7.1	1.02	
12.0	1.4	2.68	7.0	5.33	6.1	7.00	5.6	5.59	5.3	4.07	5.3	2.52	6.1	1.75	7.3	0.93	
15.0	-24.4	2.67	18.0	4.96	13.8	6.41	10.7	6.37	7.6	5.05	5.7	2.87	6.4	1.85	7.3	0.94	
18.0	-38.1	1.14	32.4	3.42	20.7	6.40	13.2	6.10	9.4	5.17	6.7	3.02	6.4	2.16	7.6	1.06	
vertical velocities in cm/s																	
x/H:	1		3		6		8		10		14		18		27		
y cm	Avg	Std	Avg	Std	Avg	Std	Avg	Std	Avg	Std	Avg	Std	Avg	Std	Avg	Std	
3.0	0.2	1.23	0.7	2.01	0.1	2.60	-0.0	2.31	0.1	1.87	0.1	1.23	-0.0	0.92	0.2	0.56	
6.0	0.5	1.36	0.2	2.70	-0.9	3.41	-1.0	2.86	-0.3	2.31	-0.3	1.65	-0.5	1.21	-0.4	0.73	
9.0	0.4	1.58	-0.1	3.12	-1.1	3.77	-1.1	3.17	-1.1	2.68	-0.4	1.69	-0.7	1.29	-0.4	0.88	
12.0	0.0	1.89	-1.8	3.32	-2.5	3.89	-1.7	3.21	-1.0	2.61	-0.7	1.73	-0.6	1.35	-0.6	0.82	
15.0	-2.8	1.78	-2.6	3.17	-2.4	3.27	-2.1	3.08	-1.4	2.48	-0.7	1.71	-0.9	1.27	-0.8	0.79	
18.0	-3.2	0.94	-3.5	1.88	-2.5	2.57	-1.9	2.43	-1.3	2.07	-1.1	1.31	-1.0	1.03	-1.0	0.64	

Situation 4, $x = 42\text{ cm} = 3H$

horizontal velocities in cm/s				
z/width:	0.25		0.75	
y cm	Avg	Std	Avg	Std
4.5	-6.9	3.12	-6.8	3.24
10	1.2	4.45	0.4	4.51
15.5	19.4	4.67	22.2	4.49
vertical velocities in cm/s				
z/width:	0.25		0.75	
y cm	Avg	Std	Avg	Avg
4.5	1.6	2.05	1.0	2.14
10	0.3	2.82	-0.4	2.85
15.5	-1.8	3.01	-1.7	2.75

Situation 4, $x = 252\text{ cm} = 18H$

horizontal velocities in cm/s				
z/width:	0.25		0.75	
y cm	Avg	Std	Avg	Std
4.5	7.5	2.04	7.0	1.83
10.0	7.1	1.61	7.5	1.84
15.5	7.1	1.80	7.4	2.12
vertical velocities in cm/s				
z/width:	0.25		0.75	
y cm	Avg	Std	Avg	Std
4.5	-0.3	1.21	-0.0	1.18
10.0	-0.7	1.32	-0.6	1.38
15.5	-0.7	1.21	-0.6	1.26

Situation 5, inflow x = -47 cm

horizontal velocities in cm/s						
z/width:	0.25		0.5		0.7	
y cm	Avg	Std	Avg	Std	Avg	Std
9.2	7.5	1.50	9.5	1.25	9.2	1.09
19.2	4.8	0.70	4.9	0.61	5.0	0.54
vertical velocities in cm/s						
z/width:	0.25		0.5		0.7	
y cm	Avg	Std	Avg	Std	Avg	Std
9.2	0.4	1.02	0.8	0.83	0.7	0.74
19.2	0.2	0.70	-0.1	0.64	-0.1	0.55

Situation 5, x = 25 cm = 1.25H

horizontal velocities in cm/s				
z/width:	0.25		0.75	
y cm	Avg	Std	Avg	Std
4.2	14.2	2.49	-2.5	1.55
14.2	2.4	3.32	-0.6	3.57
24.2	14.5	2.25	19.9	2.57
vertical velocities in cm/s				
z/width:	0.25		0.75	
y cm	Avg	Std	Avg	Std
4.2	6.3	1.18	-0.1	1.34
14.2	-2.8	2.16	-2.7	2.88
24.2	6.4	1.32	5.7	2.00

Situation 5 x = 360 cm = 18H

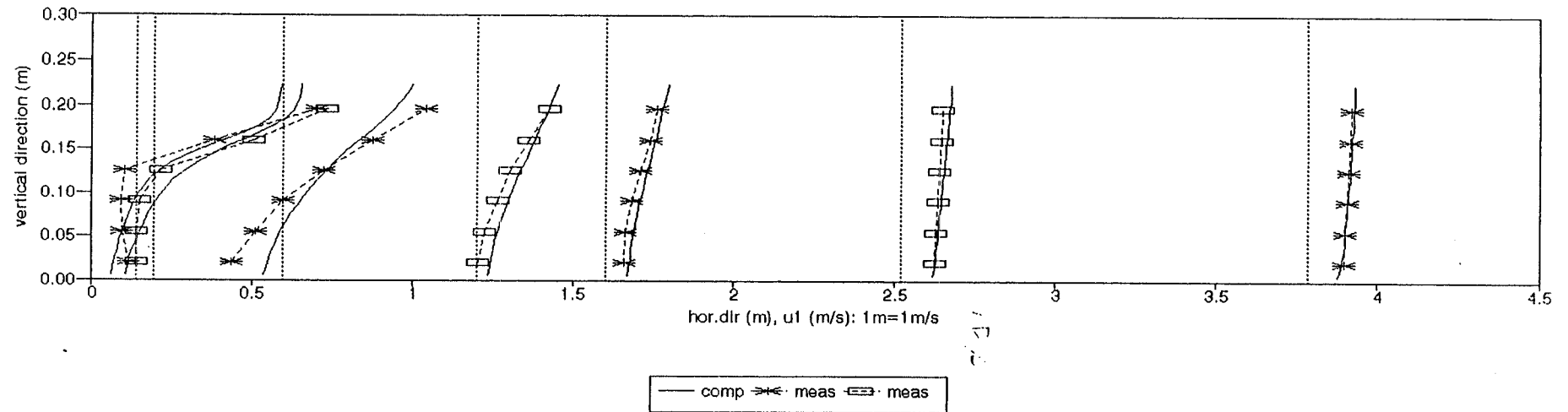
horizontal velocities in cm/s				
z/width:	0.25		0.75	
y cm	Avg	Std	Avg	Std
4.2	8.3	1.89	8.1	2.02
14.2	9.1	2.12	9.5	2.22
24.2	9.9	2.23	11.7	2.68
vertical velocities in cm/s				
z/width:	0.25		0.75	
y cm	Avg	Std	Avg	Std
4.2	0.4	1.22	0.5	1.34
14.2	0.1	1.70	0.2	1.81
24.2	-0.1	1.42	-0.1	1.56

Situation 5, flow $z = 1/2$ width

horizontal velocities in cm/s																
x/H:	0.5		0.75		1.25		1.5		2		4		10		18	
y cm	Avg	Std	Avg	Std	Avg	Std	Avg	Std	Avg	Std	Avg	Std	Avg	Std	Avg	Std
4.2	-8.9	2.30	5.4	1.29	16.8	2.35	6.7	3.98	2.9	2.76	-1.3	2.80	6.6	3.90	9.5	2.29
8.2	-3.2	1.27	2.0	1.46	13.6	2.07	11.3	2.98	6.0	2.88	2.1	2.86	9.4	4.12	10.5	2.51
12.2	-0.9	1.37	-0.3	1.46	-4.4	1.83	0.1	4.53	6.4	2.57	7.3	3.98	11.4	4.64	11.2	2.58
16.2	1.1	1.34	2.3	1.46	12.0	5.39	-4.4	2.74	6.5	2.13	14.4	4.81	13.9	5.09	11.8	2.84
20.2	6.1	1.68	14.1	2.23	20.2	2.65	14.8	4.31	14.5	4.28	22.6	4.76	16.8	5.00	11.9	2.67
24.2	42.6	1.32	34.5	0.85	13.2	2.89	37.4	2.68	35.7	3.46	29.6	3.52	19.7	4.53	12.6	2.68
vertical velocities in cm/s																
x/H:	0.5		0.75		1.25		1.5		2		4		10		18	
y cm	Avg	Std	Avg	Std	Avg	Std	Avg	Std	Avg	Std	Avg	Std	Avg	Std	Avg	Std
4.2	-0.1	2.31	-11.1	3.31	6.0	2.26	1.3	2.05	0.1	1.37	1.0	1.77	-0.4	2.48	0.4	1.35
8.2	-0.1	1.69	-13.1	2.87	-9.1	2.66	6.2	2.78	1.7	1.69	0.1	1.96	-1.5	3.01	-0.1	1.71
12.2	-0.4	1.56	-8.0	2.16	-4.0	1.74	5.0	4.73	3.0	1.89	-0.8	2.55	-1.7	3.30	-0.3	1.88
16.2	-0.7	1.52	-11.1	1.92	6.9	2.36	-1.6	3.45	2.4	3.03	-1.4	2.97	-1.7	3.04	-0.2	1.98
20.2	-0.2	1.86	-17.0	1.79	-3.2	2.86	-1.2	3.12	-0.1	3.29	-1.8	2.73	-1.8	2.83	-0.1	1.86
24.2	-4.8	0.82	-14.3	0.91	4.7	1.85	1.9	3.53	-0.0	2.57	-1.4	2.07	-1.3	2.25	-0.1	1.64

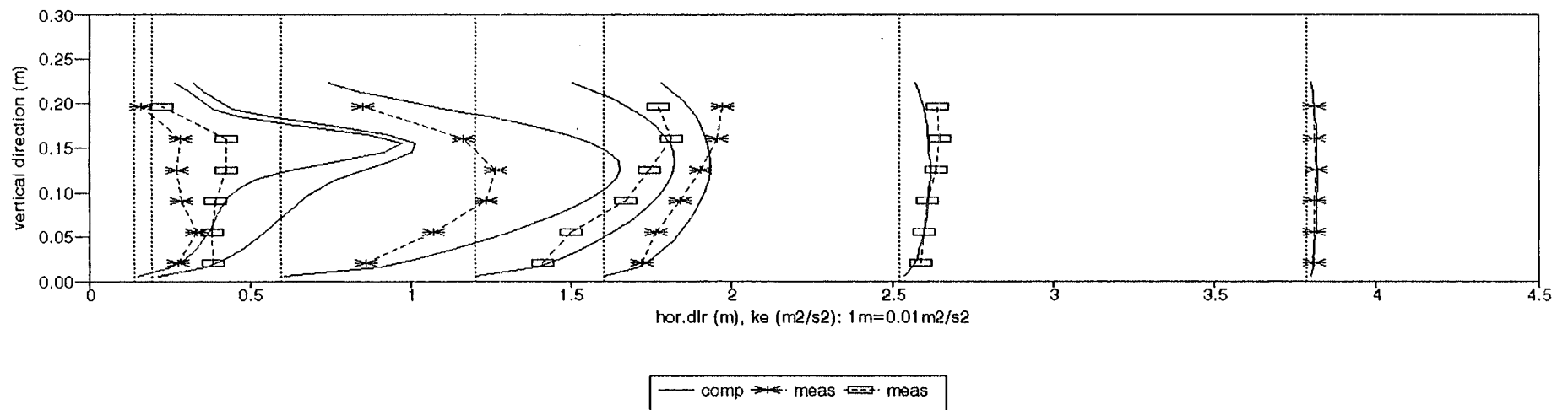
Comp. <--> meas. horizontal velocities

situation 3



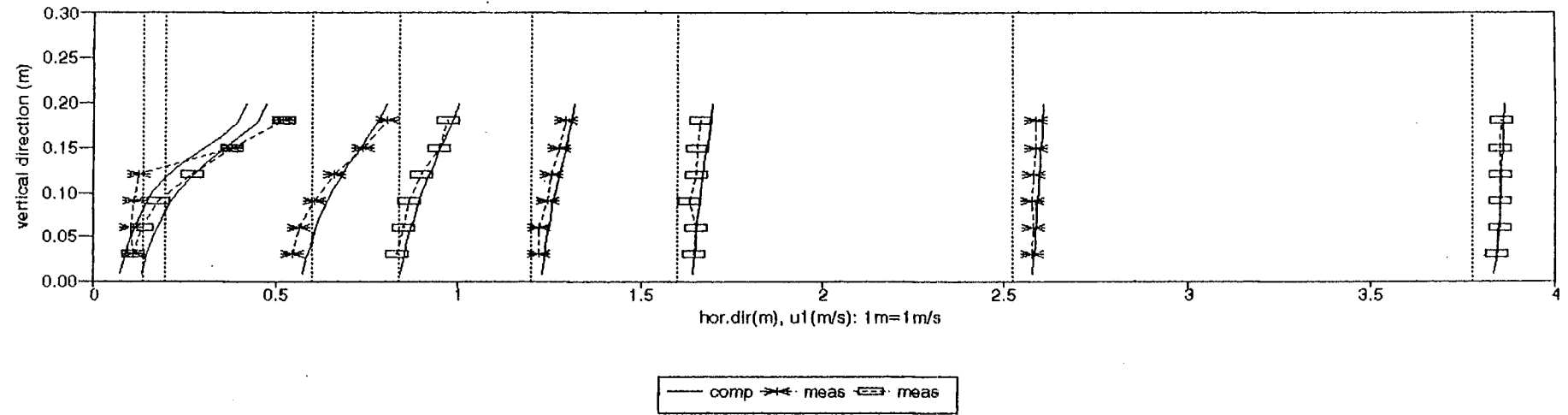
Comp. <--> meas. turbulent kin. energy

situation 3



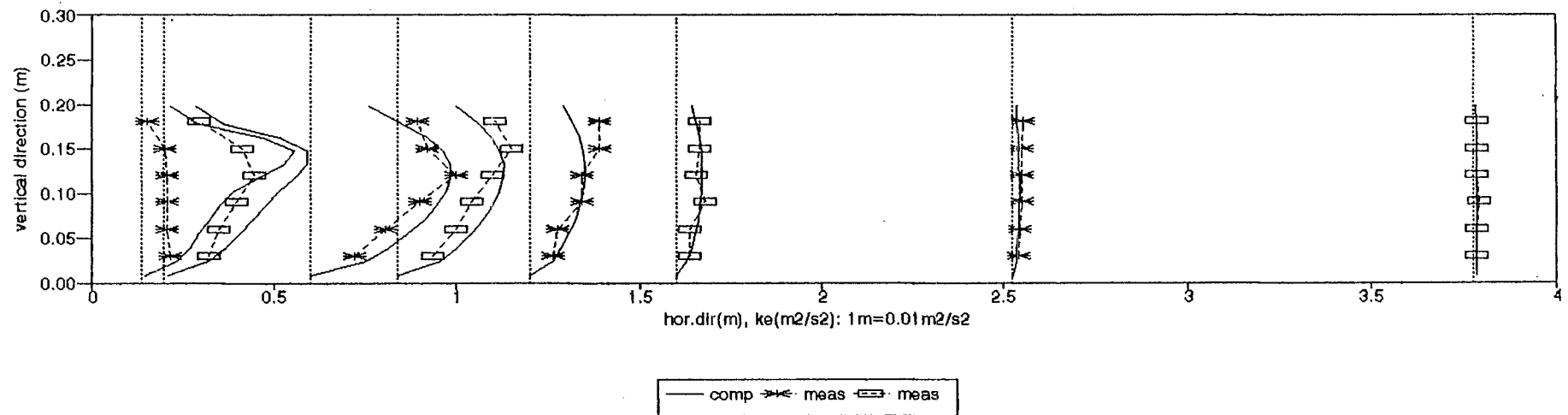
Comp. <--> meas. horizontal velocities

situation 4

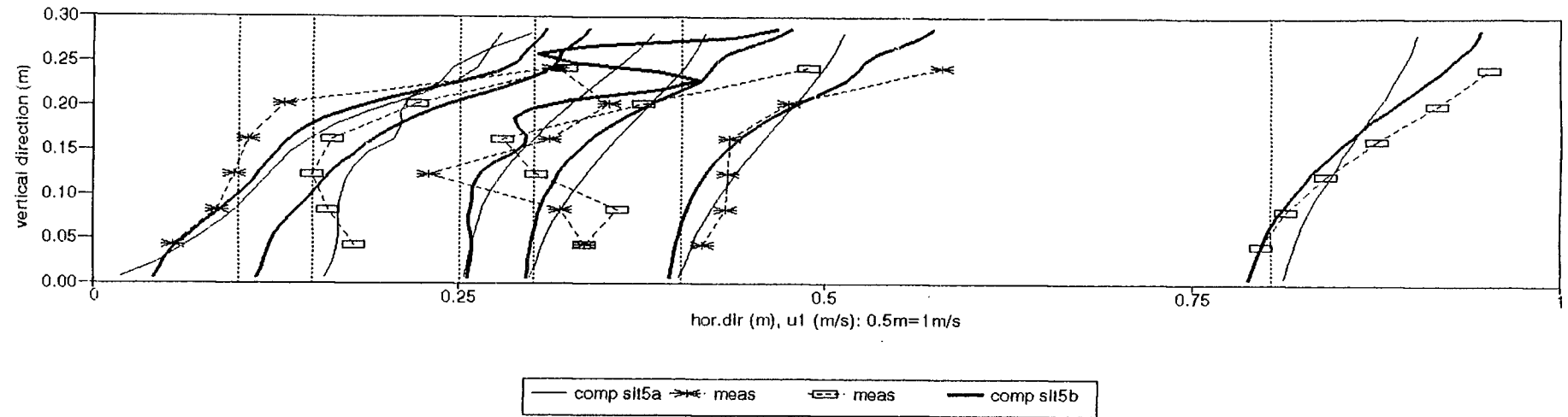


Comp. <--> meas. turbulent kin. energy

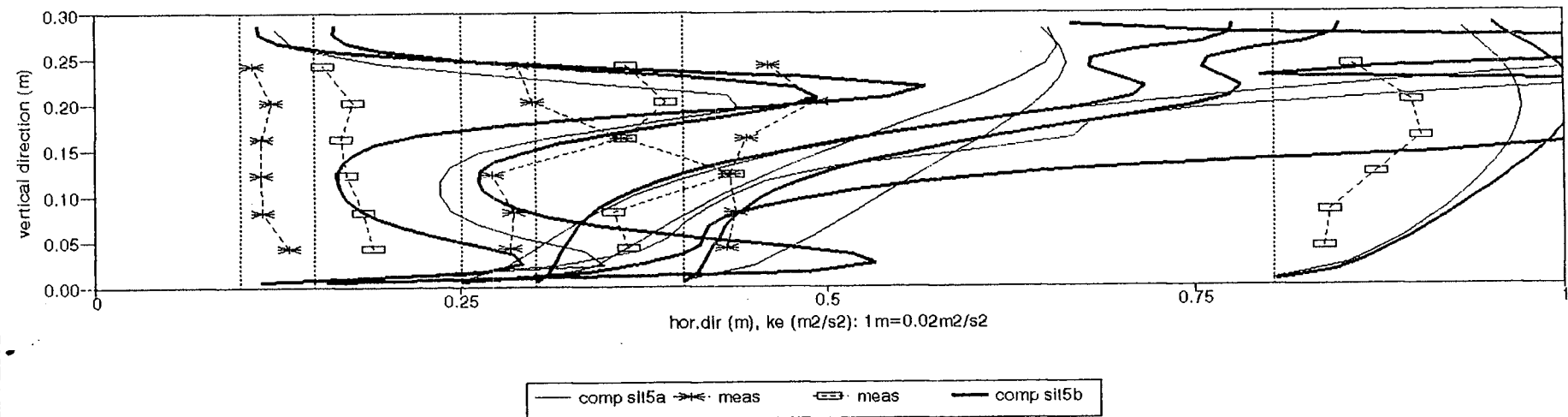
situation 4



Comp. <--> meas. horizontal velocities situation 5

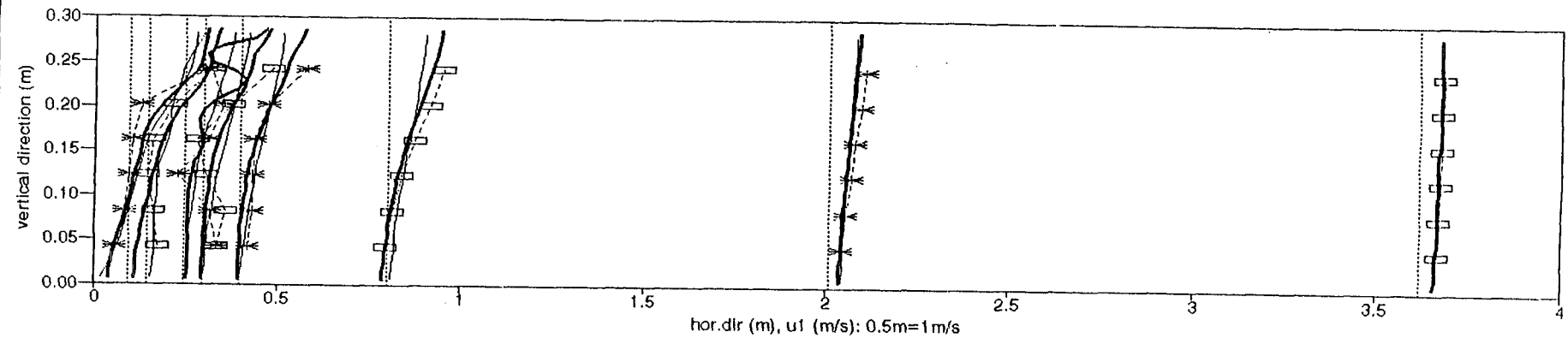


Comp. <--> meas. horizontal velocities situation 5



Comp. <--> meas. horizontal velocities

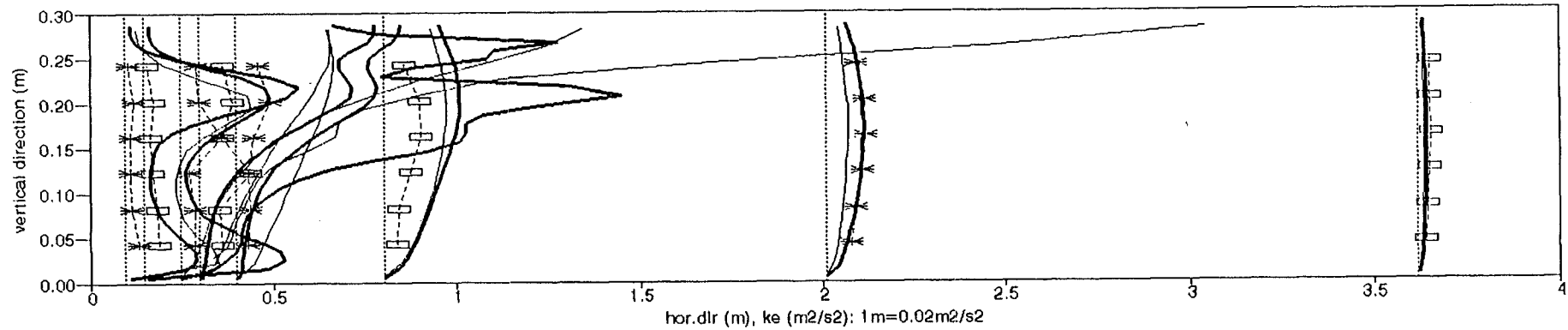
situation 5



— comp sli5a * meas □ meas — comp sli5b

Comp. <--> meas. horizontal velocities

situation 5



— comp sli5a * meas □ meas — comp sli5b

